Solution-Processed Charge Injection Layers for Organic Diodes

Master thesis

By:

Ameneh Najafi

Supervisors:

Prof. Dr. Ir. P. W. M. Blom

Drs. Ir. G.A.H. Wetzelaer

July 2012

Molecular Electronics, Physics of Organic Semiconductors

Zernike Institute for Advanced Materials

University of Groningen

Abstract

In the past decades, polymer light-emitting diodes (PLEDs) have received much attention due to their potential for easy fabrication of flexible full-color displays and lighting applications. One of the most important steps in the light generation process is the injection of charges: inefficient charge injection will strongly limit the device performance. For efficient charge injection, it is necessary to have a good alignment of both electrodes with the respective energy levels of the light-emitting polymer. In order to fully exploit the ease of fabrication of PLEDs, e.g. ink-jet printing in a roll-to-roll process, all layers are required to be solution processable. In this project, the solution-processable electron injection layer, which is a novel electron injection material called caesium stearate is investigated. Experiments have been performed with electron only diodes and light emitting diodes. Results of a broad series of electrical measurements of all-solution processed organic light-emitting diodes with different polymers are presented. The performance of these devices are compared to the standard OLED with Ba cathode. It is shown that CsSt layer spin coated from ethanol solution can be introduced as an efficient electron injector in single layer OLEDs based on red/ blue/ white emitting polymer. For the polymers used in this work comparable conversion efficiencies of the under investigation devices and conventional Ba based OLEDs can be achieved. However, the comparison of the ambient stability of the under study samples with that of Ba based device implies different degradation mechanism of OLEDs. Moreover, electron injection from CsSt has been studied with different encapsulating contact layers. It is found that devices are relatively sensitive to the choice of capping metal.

In addition, a double layer solution-processed OLED together with a single layer one including an electron transporting layer is studied as well. Although the results of single layer device presented comparable results with Ba based LED, CsSt is recommended as a better option for solution-processed cathode purposes due to easier reproducing process.

Contents

Chapter 1: Introduction

1.1Introduction

In the last several decades organic semiconductors have opened a new window in the world of technology. Since the discovery of conductivity in the polymer semiconductors [1], a new generation of electronic devices based on organic materials has been extensively investigated. In addition to the cheap and easy processing advantages of organic semiconductors with respect to inorganic ones, which is an attractive feature for marketing, organic based electronic devices hopefully may enables to fabricate flexible and transparent devices. That is why recently scientists have strongly concentrated on fabricating devices such as organic field effect transistors (OFETs), which could serve as the main component in cheap and flexible electronic circuits [2,3], organic solar cells [4,5], that may bring cheap, mass-producible and relatively efficient energy sources to the market, and organic light emitting diodes (OLEDs), the promising candidates for flexible full-color displays and lighting applications [6,7].

Organic light-emitting diodes (OLEDs) have been studied vastly since the discovery of electroluminescence in poly(*p*-phenylene vinylene) (PPV) [8]; a conjugated polymer exhibiting semiconducting property. In this category of light-emitting diodes, organic semiconductors are employed as an active or emissive layer due to their unique electronic properties which combine the electrical property of conventional inorganic semiconductors and the versatility of organic chemistry. However, organic based LEDs provide lower efficiency in comparison to inorganic LED performances. This deficiency stems from the fact that most conjugated polymers have relative low mobility, and in the

case of OLEDs the unbalanced charge transport property of conjugated materials is an additional factor which has to be considered. In this respect, there are a lot of attempts to render OLEDs competitive with inorganic ones [9-14]. Although the so far fabricated OLEDs are not as efficient as inorganic LEDs, they have a great potential in producing inexpensive large area flexible full-color displays which is inaccessible with single crystal structure inorganic materials that used in conventional inorganic LEDs. The abovementioned peculiarity is a remarkable advantage of OLEDs over inorganic LEDs, which makes them as of particular interesting research field.

Two different types of OLED fabrication routes are realized based on the class of materials or the applied technical method for depositing them. One type corresponds to the small molecule OLEDs, in which the device is fabricated via evaporation of low molecular weight molecules under high vacuum. The other one is related to the solution-based polymer LEDs, concerning all types of organic semiconductors including small molecules, oligomers, polymers and nanoparticles that can be deposited by solution-based methods such as spin coating. The disadvantage of the former method is that thermal evaporation requires relatively expensive vacuum technology, while the latter is a promising route in low-cost fabrication of large-area devices. Therefore, recently, a solid consideration is focused in the solution processing technique, which is also the interest of this project. Many efforts have been done to synthesize new materials that exhibit sufficient charge transport as well as being solution processable [9-14], although there are still big challenges to overcome the limitations of this method. The most important problem in preparation of solution-processed multilayer OLEDs can be summarized as follows: the bottom layer, in most of the cases, can be affected by the solution of subsequent layer. Therefore, many attempts have been devoted to propose a general solution for this problematic process. One approach is using intermediate liquid buffer layer to separate layers with different functions [15-17]. Example of such materials are glycerol and 1,2-propylene glycol [15]. They have high protection capability due to the high viscosity, which arises from hydrogen bonding. Using water/alcohol soluble polymers or salts is another approach to fabricate solution based multilayer OLEDs. Along these lines, a series of triphenylamine-based conjugated polyelectrolytes were reported as effective hole transporting materials [18-20]. Alternatively, for the first time Cao and coworkers introduced amino-/ammonium-functionalized polyfluorene as electron transporting material and pointed to the water/alcohol soluble property of this material [18, 21-24]. Other efforts in this area can be found in Refs [25-28]. Another suitable method to prevent erosion or mixing of the interfaces in solution-processed OLEDs is to employ cross-linkable materials. These materials consist of special agent groups, which, after being exposed to ultraviolet (UV) irradiation, create an insoluble network. Using this approach, there are many reports on

the synthesis of conjugated polymers that include reactive agents, to create optimal conditions for cross-linking [9-13].

Although numerous studies have been done to improve multilayer solution-processed OLEDs, a fully solution-based OLED has still not been achieved. In addition to the hole transport layer (HTL), emissive layer (EML) and electron transport layer (ETL), an organic light-emitting diode includes electrodes. In conventional OLEDs typically a transparent and conductive indium tin oxide (ITO) used as an anode and a low work-function metal formed via vacuum deposition technique is used as a cathode. To realize a fully solution-based OLED, the electrodes should also be fabricated from solution-processable materials whose performances are comparable with the efficient traditional ones. An important point is that besides low electrical resistance of these materials, a suitable work function is required, to have efficient charge injection. While Ohmic charge injection is accessible through thermally evaporated charge injection layers, providing such layers from solution is not straightforward. There are a few reports on preparing solution-processed metal cathodes suitable for OLEDs [29-31], materials such as Au, Cu and Ag are some examples in this field. Among them solution-processed Ag has been attracted more attention to play the role of cathode in future OLEDs with polymer substrates [32], however, currently there is no report on utilization of that. In our opinion, the abovementioned materials do not seem to be good candidates for cathodes because of their high work-functions and Fermi levels that make a high potential barrier for injection of electrons. Recently, caesium carbonate (Cs_2CO_3) has been introduced as a very efficient electron-injection material in OLEDs [33-36]. Notably, the solution-processed Cs_2CO_3 does not function as good as thermally evaporation processed of that [37,38].

The aim of this project is to develop a solution processed OLEDs by investigating the solution-processable electron injection layer, which is a novel electron injection material called caesium stearate (CsSt). The advantage of caesium stearate with respect to caesium carbonate (Cs_2CO_3) is that a better solubility as well as better adhesion on top of the polymer surface on which it is spin coated can be obtained, which is due to the long hydrocarbon chain on the caesium stearate. The general perspective of this work is to access an efficient electron injection from a solution-based cathode layer (CsSt) in single layer OLEDs based on red/ blue/ white emitting polymer. Chapter 2 gives short overview of organic semiconducting materials and briefly describes the device physics of organic diodes. Then the chapter is continued by explanations of fundamental theory of charge transport and charge injection in OLEDs. In chapter 3 the device fabrication and materials used in this work are presented. The experimental results are discussed in chapter 4 and finally, we end the report with a brief conclusion.

Refrences

[1] H. Shirakawa, T. Ito, and S. Ikeda, Makromol. Chem., 179, 1565 (1978).

[2] R. Rotzoll, S. Mohapatra, V. Olariu, R. Wenz, M. Grigas, K. Dimmler, O. Shchekin, and A. Dodabalapur, Appl. Phys. Lett., 88, 123502, (2006).

[3] L. S. Zhou, A. Wanga, S. C. Wu, J. Sun, S. Park, and T. N. Jackson, Appl. Phys. Lett., 88, 083502, (2006).

[4] M. Pagliaro, R. Ciriminna, and G. Palmisano, ChemSusChem, 1, 880 (2008).

[5] M. Suzuki, H. Fukagawa, Y. Nakajima, T. Tsuzuki, T. Takei, T. Yamamoto, and S. Tokito, J. Soc. Inf. Display, 17, 1037 (2009).

[6] S. Reineke, F. Lindner, G. Schwartz, N. Seidler, K. Walzer, B. Lussem, and K. Leo, Nature, 459, 234, (2009).

[7] Y. R. Sun, N. C. Giebink, H. Kanno, B. W. Ma, M. E. Thompson, and S. R. Forrest, Nature, 440, 908 (2006).

[8] J. H. Burroughes, D. D. C. Bradley, A. R. Brown, R. N. Marks, K. Mackay, R. H. Friend, P. L. Burns, and A. B. Holmes, Nature, 347, 539, (1990).

[9] R. Q. Png, P. Jon. Chia, S. Sivaramakrishnan, L. Y. Wong, M. Zhou, L. L. Chua, and P. K. H. Hoc, Appl. Phys. Lett., 91, 013511, (2007).

[10] N. Rehmann, D. Hertel, and K. Meerholza, Appl. Phys. Lett., 91, 103507, (2007).

[11] A. Charas, H. Alves, L. Alcácer, and J. Morgadoa, Appl. Phys. Lett., 89, 143519, (2006).

[12] L. ShengJian, Z. Cheng Mei, Z. Jie, D. ChunHui, W. XiaoHui, and H. Fei, Sci China Chem, 54, 1745, (2011).

[13] Ch. Zhong, Sh. Liu, F. Huang, H. Wu, and Y. Cao, Chem. Mater., 23, 4870, (2011).

[14] H. A. Al-Attara, and A. P. Monkman, J. Appl. Phys., 109, 074516 (2011).

[15] Sh. R. Tseng, Sh. Ch. Lin, H. F. Menga, H. H. Liao, Ch. H. Yeh, H. Ch. Lai, Sh. F. Horng, and Ch. Sh. Hsu, Appl. Phys. Lett., 88, 163501, (2006).

[16] Sh. R. Tseng, H. F. Menga, Ch.H. Yeh, H. Ch. Lai, Sh. F. Horng, H. H. Liao, Ch. Sh. Hsuc, and L. Ch. Lin, Synthetic Met., 158, 130, (2008).

[17] J. J. Park, T. J. Park, W. S. Jeon, R. Pode, J. Jang, J. H. Kwon, E. S. Yu, and M. Y Chae, Organ. Electron., 10, 189, (2009).

[18] Ch. Zhong, Ch. Duan, F. Huang, H. Wu, and Y. Cao, Chem. Mater., 23, 326, (2011).

[19] W. Shi, L. Wang, F. Huang, W. Yang, R. S. Liu, and Y. Cao, Polym. Int., 58, 373, (2009).

[20] W. Shi , S. Q. Fan , L. Wang , W. Yang , and Y. Cao, Acta. Polym. Sin., 5, 465, (2009).

[21] F. Huang, H. B. Wu, D. L. Wang, W. Yang, and Y. Cao, Chem. Mater., 16, 708, (2004).

[22] H. B. Wu, F. Huang, Y. Q. Mo, W. Yang, D. L. Wang, J. B. Peng, and Y. Cao, Adv. Mater., 16, 1826, (2004).

[23] F. Huang, L. T. Hou, H. B. Wu, X. H. Wang, H. L. Shen, W. Cao, W. Yang, and Y. J. Cao, Am. Chem. Soc., 126, 9845, (2005).

[24] H. B. Wu, F. Huang, J. B. Peng, and Y. Cao, Org. Electron., 6, 118, (2005).

[25] F. Huang, H. B. Wu, J. B. Peng, W. Yang, and Y. Cao, Curr. Org. Chem., 11, 1207, (2007).

[26] F. Huang, Y. Zhang, M. S. Liu, and A. K.-Y. Jen, Adv. Funct. Mater., 19, 2457, (2009).
[27] F. Huang, P.–I. Shih, C.–F. Shu, Y. Chi, and A. K.-Y. Jen, Adv. Mater., 21, 361, (2009).
[28] F. Huang, H. B. Wu, and Y. Cao, Chem. Soc. Rev., 39, 2500, (2010).
[29] D. R. Redinger, S. Molesa, S. Yin, R. Farschi, and V. Subramanian, IEEE Trans. Electron Devices, 51, 1978, (2004).
[30] T. Cuk, S. M. Troian, C. M. Hong, and S. Wagner, Appl. Phys. Lett., 77, 2063, (2000).
[31] H. D. Goldberg, R. B. Brown, D. P. Liu, and M. E. Meyerhoff, Sens. Actuators B, 21, 171, (1994).
[32] R. S. Sathish, Y. Kostov, D. S. Smith, and G. Rao, Plasmonics, 4, 127, (2009).
[33] T. Hasegawa, S. Miura, T. Moriyama, T. Kimura, I. Takaya, Y. Osato, and H. Mizutani, SID Int. Symp. Digest Technol. Papers, *35*, 154, (2004).
[34] C. I.Wu, C. T. Lin, Y. H. Chen,M. H. Chen, Y. J. Lu, and C. C.Wu, Appl. Phys. Lett., 88, 152, (2006).
[35] C. W. Chen, Y.-J. Lu, C. C. Wu, E. H. Wu, C. W. Chu, and Y. Yang, Appl. Phys. Lett., 87, 241, (2005).
[36] J. Huang, T. Watanabe, K. Ueno, and Y. Yang, Adv. Mater., 19, 739, (2007).
[37] J. Huang, G. Li, E.Wu, Q. Xu, and Y. Yang, Adv. Mater., 18, 114, (2006).
[38] G. Li, C.-W. Chu, V. Shrotriya, J. Huang, and Y. Yang, Appl. Phys. Lett., 88, 253, (2006).

Chapter 2: Theory

2.1 Introduction

Inefficient charge injection will strongly limit the device performance, especially in case of semiconductors with low mobility, it is important that the Fermi levels of the electrodes align with the HOMO and LUMO of the organic material that is used as emissive layer (EML) in a single layer OLED. Creation of interface barriers between electrodes and organic layer hinder the injection process, resulting in unbalanced charge injection, and as a consequence an excess of one type of charge carrier would decrease the conversion efficiency. Therefore, this chapter devoted to basic theoretical background governs the charge injection and charge transport processes in an OLED. First, the organic semiconductor, the active material of an OLED, is described. In the follow, organic diodes are introduced and the electrical characteristics of them are discussed as well.

2.2 Organic Semiconductor

The discovery of relatively high electrical conduction in polyacetylene doped with the halogen iodine in 1977 [1-3], which awarded with the 2000 Novel Prize in chemistry, makes the organic materials or polymers as an active elements in electronics. This special class of polymers exhibits the semiconducting properties. However, the semiconducting behaviors in organic materials like anthracene and poly(*N*-vinyl carbazole) (PVK) was studied earlier [4-8]. The alternation of single and double bonds in the structure of such organic materials, socalled conjugation, causes the

semiconducting property. In conjugation semiconductors, one carbon atom combines with two other carbon atoms and one hydrogen atom or a side group through the three sp^2 hybridized electrons in the outer shell, which results in-plane σ bonds. The fourth electron of carbon forms a P_z orbital perpendicular to the plane of σ bonds. This P_z orbital of one carbon has overlap with other P_z orbitals of neighboring carbon atoms which leads to formation of π bonds [figure 2.1(a)]. The π bond electrons are delocalized over a distance in the backbone of polymer structure, as illustrated in figure 2.1(b). The delocalized electrons fill up whole band which is called Highest Occupied Molecular Orbital (HOMO) and can excite to the empty π^*-band which is called the Lowest Unoccupied Molecular Orbital (LUMO). Therefore, the HOMO and LUMO levels resemble the valence and conduction bands in the inorganic semiconductors, respectively [figure 2.2]. The energy difference between HOMO and LUMO levels corresponds to the band gap and it is typically between 1-4 eV which covers the entire visible spectrum. After the discovery of electroluminescence in poly(*p*-phenylene vinylene) (PPV) [9], organic semiconductors considered as a good candidate for OLEDs and optoelectronic devices. Some prototypical examples of organic polymers which are used mostly in OLEDs are presented in figure 2.3. These organic polymers are easily processed from solution and the solubility and the emission color can be tuned by modifying the side groups [10].

Contrary to inorganic semiconductors, organic materials do not have well ordered energy bands. Organic polymers are very disordered materials in which the conjugation structure might be broken due to kinked and folded chains or chemical defects. So, one should think of polymers as a segments with different lengths. Every segment of different length has a different energy. The distribution of energy levels is usually approximated by a Gaussian function [figure 2.4].

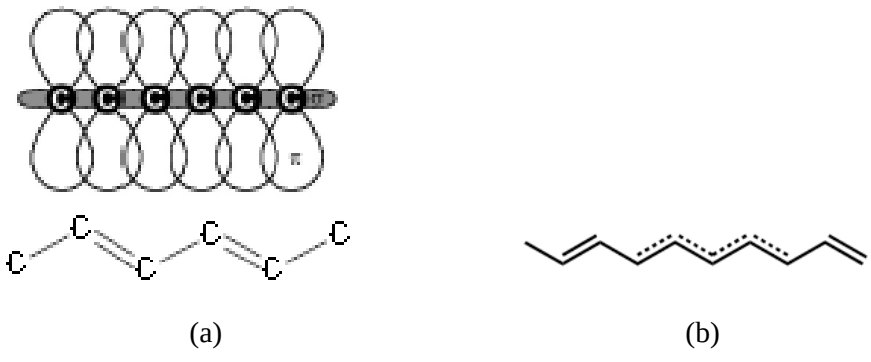

(a) (b)

Figure 2.1. (a) Schematic of conjugation in the polymer backbone, (b) extension of π bond electrons over the backbone structure.

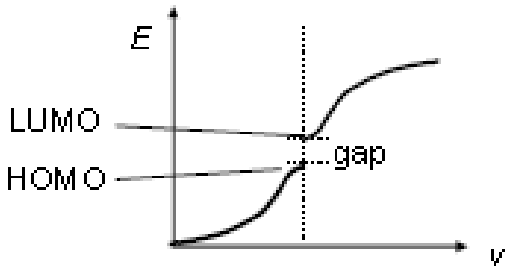

Figure 2.2. Electronic structure of an intrinsic organic semiconductor.

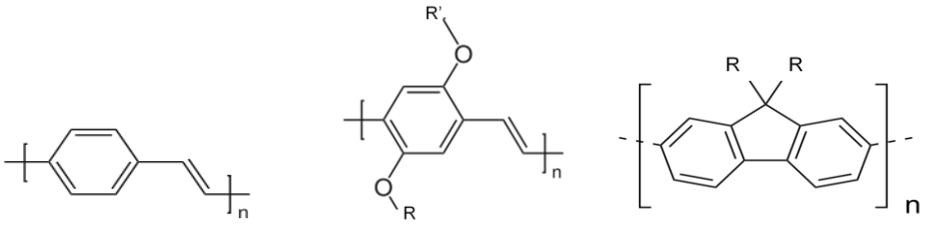

Figure 2.3. The chemical structure of (a) poly(phenylene vinylene) (PPV), (b) poly(2-methoxy-5-(2′-ethylhexoxy)-1,4-phenylenevinylene)(MEH-PPV) and (c) polyfluorene.

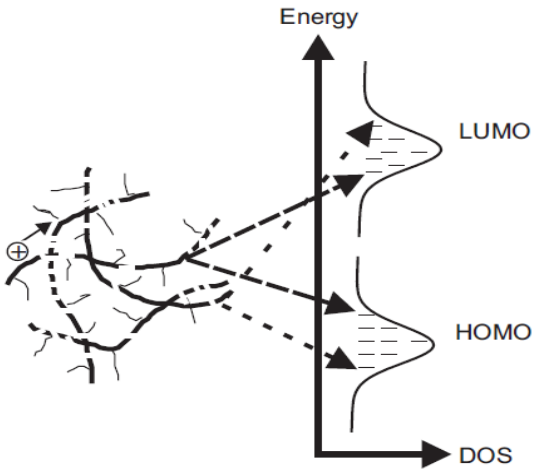

Figure 2.4. Illustration of the shape of density of states in HOMO and LUMO levels of an organic semiconductor.

Since the conjugation length is limited, electrons and holes have to hope from one localized site to the unoccupied neighboring segment site. Therefore, conduction in the organic semiconductors is dominated by the hopping mechanism. This is the main justification of less electrical conductivity of organic materials in comparison to inorganic ones. However, in contrast to inorganic semiconductors, mobility, a measure of conductivity of a material, is strongly thermally assisted in organic semiconductors. The study of mobility helps one to understand organic material characteristics. It is observed that higher mobility is resulted by increasing temperature which indicates that, with the aid of phonons, charge carriers can overcome the potential barriers to jump into unoccupied localized states in higher energy levels. Therefore, mobility is a temperature dependent parameter proceeding by the hopping which initially described by Miller and Abrams [11]. Further transport measurements of organic devices have shown that charge carrier mobility depends not only on temperature but also on the applied electric field together with charge carrier density [12].

2.3 Organic Diodes

A simple design of organic diode consists of a single layer of organic semiconductor material sandwiched between two electrodes. Depending on the materials which are used as electrodes, three different types of diodes are achieved as illustrated in figure 2.5. Two of them are known as single carrier devices, since they allow only one type of charge carrier, electron or hole, transfer through the device. These diodes are used to study the charge transport in organic semiconductors. In a single carrier diode, one of the electrodes is selected in such a way that it produces a large potential barrier for unwanted charge carrier, so the current in the device is provided by injection of favorable charge carrier from the other electrode that has a good alignment of work-function with HOMO (hole only device) or LUMO (electron only device) of the active layer [figures 2.5(a) and (b)]. The third type of diodes is a light emitting diode in which electrons are injected from cathode and holes are injected from anode into the LUMO and HOMO level of organic semiconductor, respectively. The charge carriers move toward each other and due to the coulomb interaction they attract each other which results in the formation of excitons. The formation of excitons is followed by emission of light which is due to a so-called recombination process. Depending on the band gap of the semiconductor, the light output may be created in a region of the visible spectrum. The abovementioned processes that govern the operation of OLEDs are shown schematically in figure 2.5(c).

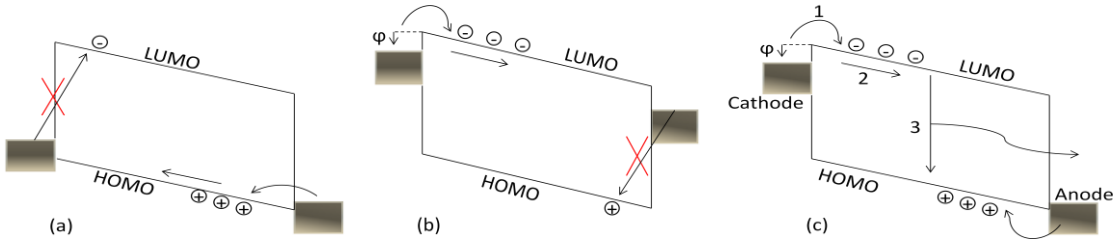

Figure 2.5. Design of single-layer organic diodes: (a) hole only diode, (b) electron only diode, and (c) light emitting diode together with illustration of basic operating processes of OLEDs; 1- charge injection, 2- charge transport and 3- recombination.

2.4Electrical Characteristics of OLEDs

The process of luminescence in organic light emitting diodes is under the influence of complexes electronic procedures; charge injection and charge transport through the devise. The process of entering charge carriers into the active layer is referred to as charge injection since the carriers enter through the surface boundary. Depending on the potential barrier at the interface the current might be either charge injection limited or bulk limited. In practical diode thicknesses if the injection barrier $\varphi \leq 0.3$ eV the current is limited by bulk transport [13], otherwise the charge transport rate in the active layer is higher than the injection rate, then the electrode cannot supply as a reservoir anymore and the current becomes limited by injection. Additionally, in the case of light emitting diodes the unbalanced charge injection also gives rise to a large decrease of the conversion efficiency. This section is mostly inspired of Refs [14 and 15].

2.4.1 Charge Injection

A formation of interface barrier between semiconductor and metal contact is illustrated in figure 2.6. Before contact two systems are in their original states (left picture in figure 2.6). Upon contact, the Fermi levels of metal and semiconductor line out, as a result, the band bending appears in the orbital levels of semiconductor. Then, the interface energy barrier is the energy that charge carriers need to go from the Fermi level of the metal into the conduction level (LUMO level in organic semiconductors) of the semiconductor after the contact; $\phi_b = E_c - E_F$. By comparing the work-function of metal (ϕ_M) and work-function of semiconductor (ϕ_S) three different types of contact barrier would be resulted as shown in figure 2.7. If the metal work-function is larger than semiconductor work-function ($\phi_M > \phi_S$), electrons would be depleted from semiconductor, so the contact region cannot supply enough charge carriers to the bulk of the semiconductor

and the contact is called injection limited for electrons while it is ohmic for holes [figure 2.7(a)]. Under the condition of figure 2.7(b) the Fermi levels and, as a consequence, the work-functions are equivalent, therefore no redistribution of charge carriers is needed. When the metal work-function is smaller than that of semiconductor ($\phi_M < \phi_S$), electrons flow from metal to the semiconductor and holes are accumulated at the interface, as a result the contact is ohmic for electrons and at the same time it is injection limited for holes [figure 2.7(c)].

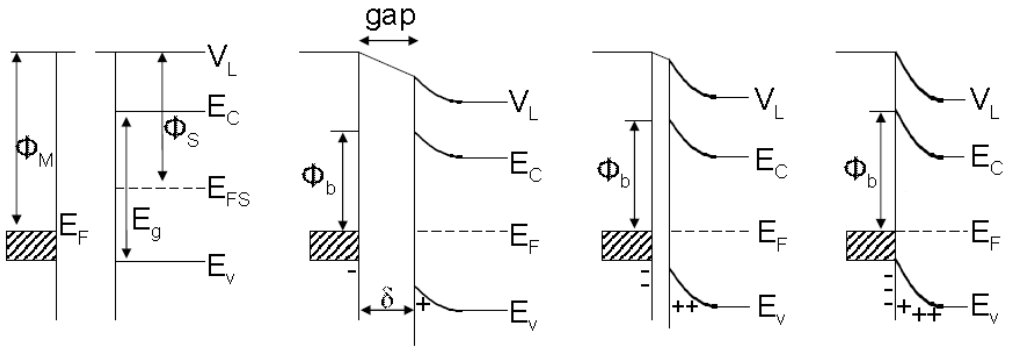

Figure 2.6. Interface barrier formation between a metal contact and semiconductor.

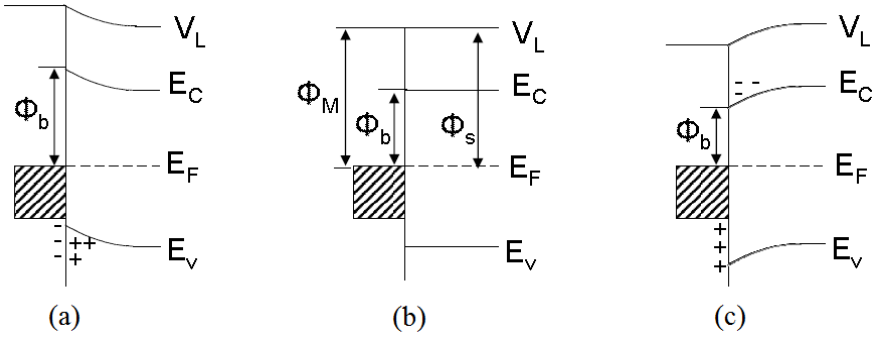

Figure 2.7. Different barrier types upon the contact of a metal and semiconductor. (a) describes the condition of $\phi_M > \phi_S$ where the contact is injection limited for electrons and it is ohmic for holes, (b) corresponds to a neutral contact $\phi_M = \phi_S$, and (c) shows the ohmic contact for electrons and injection limited situation for holes ($\phi_M < \phi_S$).

In an OLED a high work-function material such as poly(3,4-ethylenedioxythiophene) doped with poly(styrenesulfonate) (PEDOT-PSS) and a low work-function material, like Barium (Ba), are chosen as two electrodes. After connection, at zero voltage, the Fermi levels line out by flowing electrons through the external circuit from the cathode (Ba) to the anode (PEDOT-PSS) which leads to formation of a built-in electric field. This built-in electric field opposes the drift current. As long as the applied voltage is below the built-in voltage, the current is dominated by diffusion and increasing of the voltage ($V > V_{bi}$) leads to fully surmounting the built-in field and providing the situation of recombination. These situations are depicted in figure 2.8.

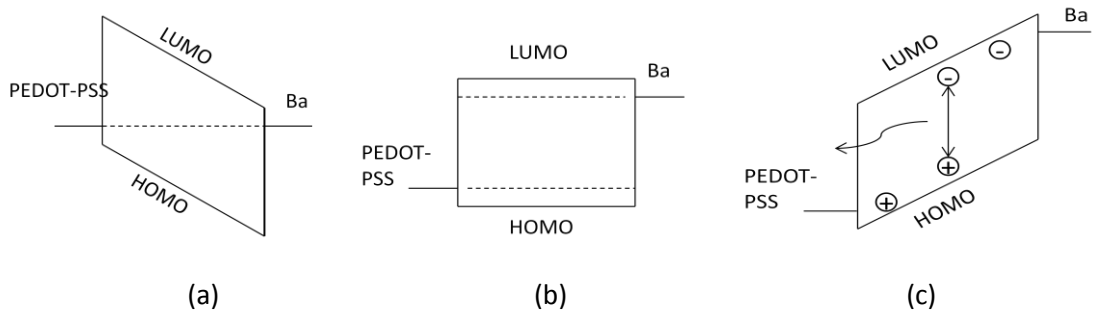

Figure 2.8. Illustration of band diagram of an OLED with ohmic contacts at (a) no applied bias (V=0), (b) when $V=V_{bi}$, and (c) $V>V_{bi}$.

2.4.2 Current-Voltage Characteristics

The main feature of current-density-voltage (J-V) characteristic of an organic LED is being non-linear, which is associated with the fact that the driving current is due to the injection of charge from the electrodes and not resulted from the bulk-generated carriers [16]. Whenever the ohmic contacts are formed by the appropriate electrodes in an OLED, three different regimes can be distinguished in a plot of J-V measurements: 1) leakage, 2) diffusion and 3) space charge limited current (SCLC) regimes. This feature is observed for a typical OLED device in figure 2.9. From figure, at low voltages the current is dominated by leakage current. Leakage current behaves linearly with increasing voltage up to a certain amount of voltage which is here approximately 1.6 eV. Above 1.6 eV, the dependence of density current on the voltage changes from linear to the exponential trend, which is known as diffusion regime. At higher voltages, above built-in voltage, the behavior of current verses voltage tends to a quadratic dependence and reaches the maximum value in high biases so-called space charge limited regime.

So, one can use a J-V plot to estimate the built-in voltage at which the current starts to deviate from the exponential behavior. In this example it is ~2.2 eV apparent in the figure.

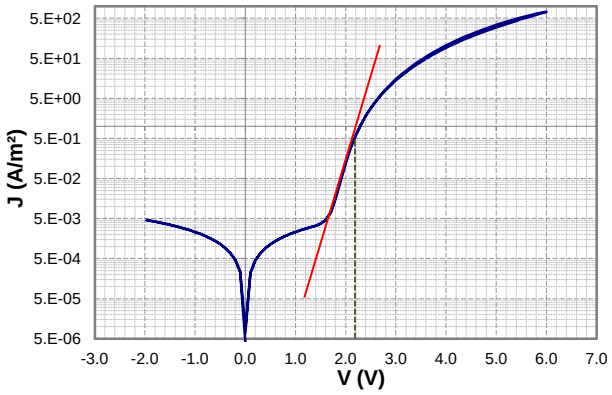

Figure 2.9. An example of typical J-V measurements of an OLED.

2.5 Summary

In summary, organic semiconductors were introduced as prominent materials in new technologies such as OLEDs. It was explained that the semiconducting property of organic semiconductors stems from the alternation of single and double bonds in the backbone. Organic polymers are disorder materials in which the conduction is dominated by the hopping mechanism which is temperature assisted. These organic polymers are easily processed from solution and enable to proceed solution processable OLEDs.

The charge injection, one of the important processes of OLED operation, was described in detail. The importance of alignments between the work-function of electrodes and the HOMO and LUMO levels of active layer in an OLED was highlighted. The nonlinearity characteristics of current-density-voltage of OLEDs, an electric field dependent quantity including leakage, diffusion and space-charge limited current, was shown using an example of J-V measurements of a typical OLED.

By considering the fundamental concepts mentioned in this chapter we use a novel solution processed electron injector material in our experiments. The results of our investigations will be discussed in the following chapters.

Refrences

[1] H. Shirakawa, E. J. Louis, A. G. MacDiarmid, C. K. Chiang, and A. J. Heeger, J. Chem. Soc., Chem. Commun., 16, 578 (1977).

[2] C. K. Chiang, C. R. Fincher, Y. W. Park, A. J. Heeger, H. Shirakawa, E. J. Louis, S. C. Gau, and A. G. MacDiarmid, Phys. Rev. Lett., 39, 1098 (1977).

[3] C. K. Chiang, M. A. Druy, S. C. Gau, A. J. Heeger, E. J. Louis, A. G. MacDiarmid, Y. W. Park, and H. Shirakawa, J. Am. Chem. Soc., 100, 1013 (1978).

[4] M. Pope, H. P. Kallmann, and P. Magnante, J. Chem. Phys., 38, 2042 (1963).

[5] W. Helfrich and W. G. Schneider, Phys. Rev. Lett., 14, 229 (1965).

[6] H. Hoegl, J. Phys. Chem., 69, 755 (1965).

[7] D. M. Pai, J. Chem. Phys., 52, 2285 (1970).

[8] W. D. Gill, J. Appl. Phys., 43, 5033 (1972).

[9] J. H. Burroughes, D. D. C. Bradley, A. R. Brown, R. N. Marks, K. Mackay, R. H. Friend, P. L. Burns, and A. B. Holmes, Nature, 347, 539 (1990).

[10] A. C. Grimsdale, K. Leok Chan, R. E. Martin, P. G. Jokisz, and A. B. Holmes, Chem. Rev., 109, 897 (2009).

[11] A. Miller and E. Abrahams, Phys. Rev., 120, 745 (1960).

[12] W. F. Pasveer, J. Cottaar, C. Tanase, R. Coehoorn, P. A. Bobbert, P. W. M. Blom, D. M. de Leeuw, and M. A. J. Michels, Phys. Rev. Lett., 94, 206601 (2005).

[13] P. W. M. Blom, and M. C. J. M. Vissenberg, Mater. Sci. Eng., R 27, 53, (2000).

[14] T. van Woudenbergh, Zernike Institute PhD thesis, ISBN: 90-367-2277-2, (2005).

[15] H. T. Nicolai, Zernike Institute PhD thesis, ISBN: 978-90-367-5398-2 (Electronic version), (2012).

[16] J. Kalinowski, Marcel Dekker, New York, U.S.A, ISBN: 0-8247-5947-8, (2005).

Chapter 3: Device structure and Characterization Technique

3.1 Introduction

In the current chapter, the design of the device and the experimental procedures for fabrication and characterization of that are described. Also, the materials used throughout this research are introduced in the follow.

3.2 Device Fabrication and Electrical Measurements

An illustration of the under study OLED devices is presented in figure 3.1. As mentioned before, the purpose of this project is to investigate the solution-based OLEDs which can be fabricated by spin coating method. Therefore, the materials that are used in such LEDs are organic materials with typical low conductivity which necessitate the fabrication of very thin layers of the order of 100 nm. Dust particles are detrimental for operation of such nano-scale layers, so whole the fabrication procedures have been done in cleanroom environment. The samples were processed on top of $3 \times 3\ cm^2$ glasses patterned by indium tin oxide (ITO) layer. After cleaning substrates in the wet station ultrasonically by acetone and propanol, they were dried in oven at $140℃$ for 10 minutes and subsequently exposed to ultraviolet (UV) irradiation. However ITO is a suitable transparent conductor allowing the generated light to escape through the bottom contact, it is not smooth enough and spikes of that may pierce through the active layer and create shorts. In addition, the work function of ITO tends to be decreased with time. In order to

overcome these unexpected side effects, a conjugated polymer poly(3,4-ethylenedioxythiophene) doped with poly(styrenesulfonate) (PEDOT-PSS) was used as a flattening layer which prevents current leakage caused by local shorts, and improves the work function as well. The spin coated PEDOT-PSS layer was typically 60 nm in thickness. In order to remove the remaining water, samples were backed at 140℃ and then the next steps were following inside the nitrogen-filled glovebox.

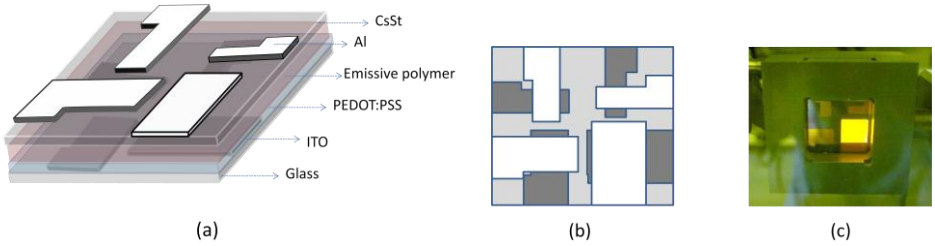

Figure 3.1. Configuration of OLED samples; (a) an illustration of different layers, (b) the top view, and (c) the OLED under operation.

A series of polymers from red to the blue luminescent, consisting MEH-PPV, NRS-PPV, SPB103-001, SPB001-002 and SPW106, were spin coated from solution as an emissive layer. All polymers, except MEH-PPV, were dissolved in Toluene and MEH-PPV was dissolved in chlorobenzene. The program which used to spin coat them was set at 1000 rpm. In the last step, a new salt of caesium that is synthesized from stearic acid and caesium carbonate [figure 3.2] was spin coated as well, from ethanol solution, and finally, the cathode was capped with 100 nm aluminum. The capping layer was deposited through the mask using thermal evaporation technique under the chamber pressure 10^{-6} mbar. The overlap of bottom (ITO) and top (Al) contacts defines four active areas in each device, ranging from $\sim 1 \times 10^{-5}$ m^2 to $\sim 1 \times 10^{-4}$ m^2. It is schematically shown in figure 3.1(b), and an example of OLED under operation can be seen in figure 3.1(c).

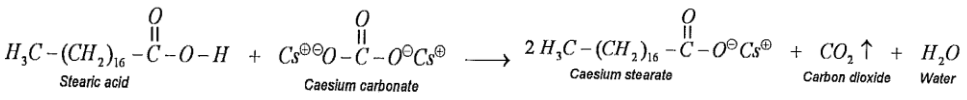

Figure 3.2. The Synthesis of the caesium stearate (CsSt).

In this thesis several different structures of OLEDs were investigated, like single-carrier devices or inverted one, via replacing the anode and cathode by other appropriate electrodes of which we will mention to them in the next chapter.

The current-voltage measurements were performed in the nitrogen-filled glove box using a computer controlled Keithley 2400 SourceMetere and the emission spectra were collected via a Si-photodiode connected to a Keithley 6514 electrometer. Thicknesses were measured by a Dektak 6M Stylus Profiler.

Chapter 4: Results and discussion

4.1 Introduction

In this chapter the results of our experimental data of studying OLEDs, in which CsSt is employed to play the role of electron injector, are presented. It is demonstrated that CsSt can act as an effective cathode for single layer conventional OLEDs based on variety of luminescent polymers. Afterward, a short study on an electron transporting material called LP121-F4, a polyfluorene derivative, is treated and a brief conclusion is provided at the end of this chapter.

4.2 Solution processed electron injection layer; CsSt

OLEDs based on series of polymers with different band gaps and characteristics are discussed in this section. Different device configurations are investigated. In all the OLEDs the ITO electrode covering by PEDOT-PSS plays the role of anode and CsSt is considered as cathode, unless we point to that where the device has different structure than the conventional ones. To clarify our results we compare them with a reference device in that Ba is employed to inject the electrons into the LUMO level of active material instead of the case study cathode, i. e. CsSt. Barium, a metallic material which has to be deposited through the thermal evaporation technique, has a low work-function close to 2.6 eV introducing it as a good electron injector for a broad variety of polymers. First the results of PPV derivative based LEDs are presented, and then the devices with two types of blue polymers (SPB001-002 and SPB103-001) and a white copolymer (SPW106) active layers are studied.

4.2.1 Charge injection and recombination in derivatives of poly(*p*-phenylene vinylene)(PPV)

First, the results of a conventional OLED consisting 150 nm poly(4'-(3,7-dimethyloctyloxy)-1,1'-biphenylene-2,5-vinylene) (NRS-PPV) emitting layer are discussed. NRS-PPV is a well-studied derivative of prototypical conjugated polymer called poly(*p*-phenylene vinylene)(PPV). The band gap of NRS-PPV is approximately equal to 2.2 eV, yielding a red/orange emission.

The film formation processes can affect both the thickness layer and how the layer covers the beneath layer in quality. The two important factors which in regarding to cathode layer can directly impress the charge injection at the interface layer as well as quantum efficiency (QE) (photon/charge carrier). So we tried to find the optimum spin coating program for 2 mg/ml concentration of CsSt. Among the different programs that were used, the best results were in associated with the 1000 rpm spin coating program of the cathode layer which are depicted in figure 4.1 together with the data of Ba based OLED as a reference. It can be observed that the light output and current efficiency (light output/current) of the under investigation devices are comparable with the performance of reference device over the whole applied voltages. It may imply that the contact is ohmic and there is no injection limited. However the current feature of sample with open lid coating program is more consistent with reference device and for an unknown reason the current density of sample with closed lid programming is higher than Ba based device, figure 4.1.(c) shows that the maximum efficiency of the device which is coated with closed lid condition is slightly higher than that of all devices. So, it is not clear to claim which program is better than the other. Besides the quantity of the device efficiency, the uniformity of lighting area is also of importance. For the two cases with 1000 rpm coating (open and closed lid), a uniform shining area with very tiny dark spots was seen, in contrast, the other samples with different spin coating program exhibited a nonuniform lighting with random dark parts. We may conclude that this is the reason of less efficiency belongs to the devices with higher speed coating of cathode (these results are not shown here), since larger part of the device is not active in the light-emission process, although the current also was not efficient enough.

The use of different concentration of material may lead to creation of a layer with different thickness. Here, as the same as previous one, the best results of an OLED with the cathode of 5 mg/ml CsSt were related to the 1000 rpm spin coating of cathode. In this case, as figure 4.2 indicates, the current is more sensitive to the spin coating program in comparison to the previous samples. In addition, the currents are order of magnitude lower than that of previous ones. This seems that the injection would be somewhat problematic for these samples as compared to the devices with 2 mg/ml CsSt

cathode. The reason of that is still a challenge and it is not proved to be a consequence of thickness problem. Nevertheless, the light output and efficiency of the device in which the cathode is spin coated with closed lid are comparable with the performance of reference device, especially in higher operating voltages. Since the quenching effect would be expected to be the same in all devices, so the lower efficiency in low voltages may be justified by the higher leakages in under study device.

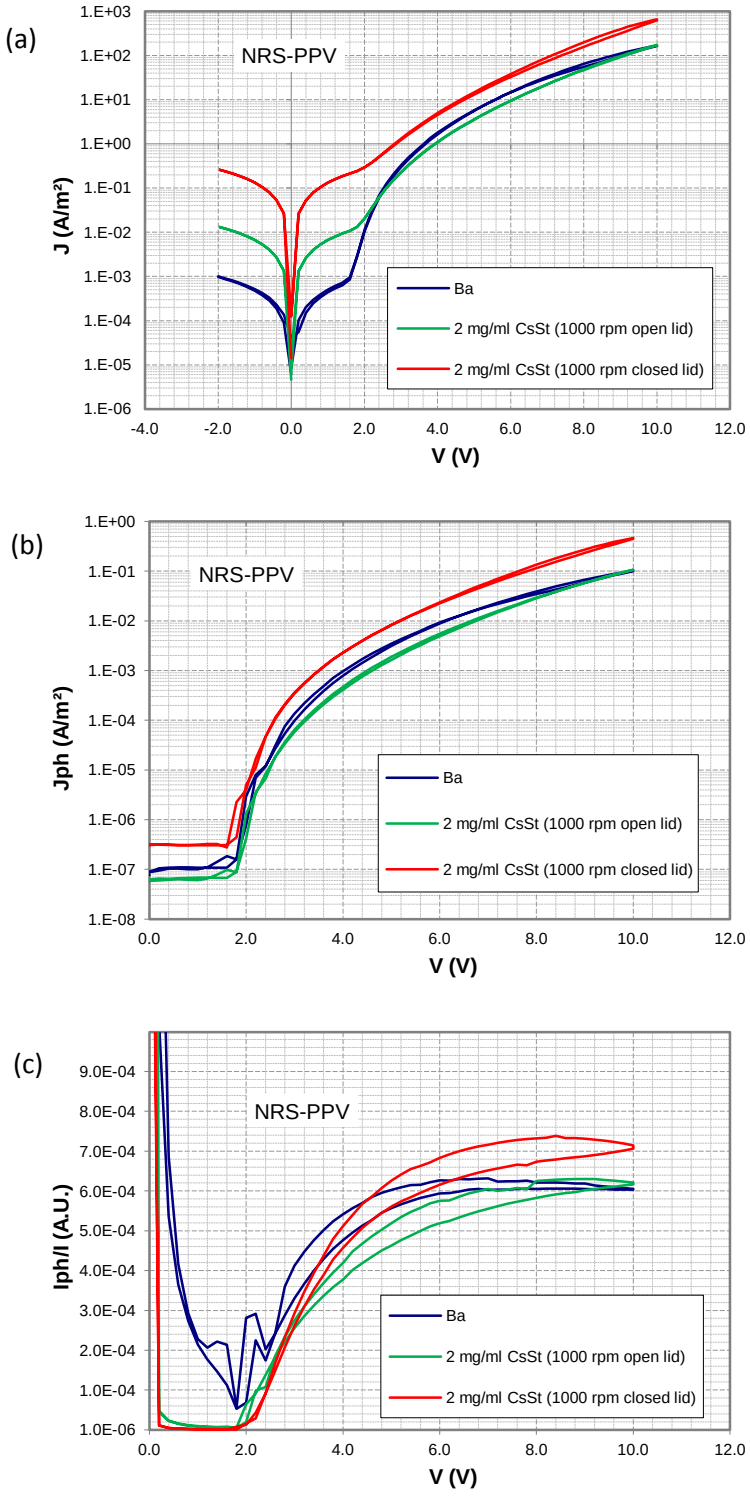

Figure 4.1. (a) J-V characteristics of OLEDs consisting 150 nm NRS-PPV (active layer) with different programs of spin coating 2 mg/ml CsSt as a cathode at room temperature compared to the device with Ba cathode (blue line). The corresponding (b) photocurrent density and (c) efficiency of devices.

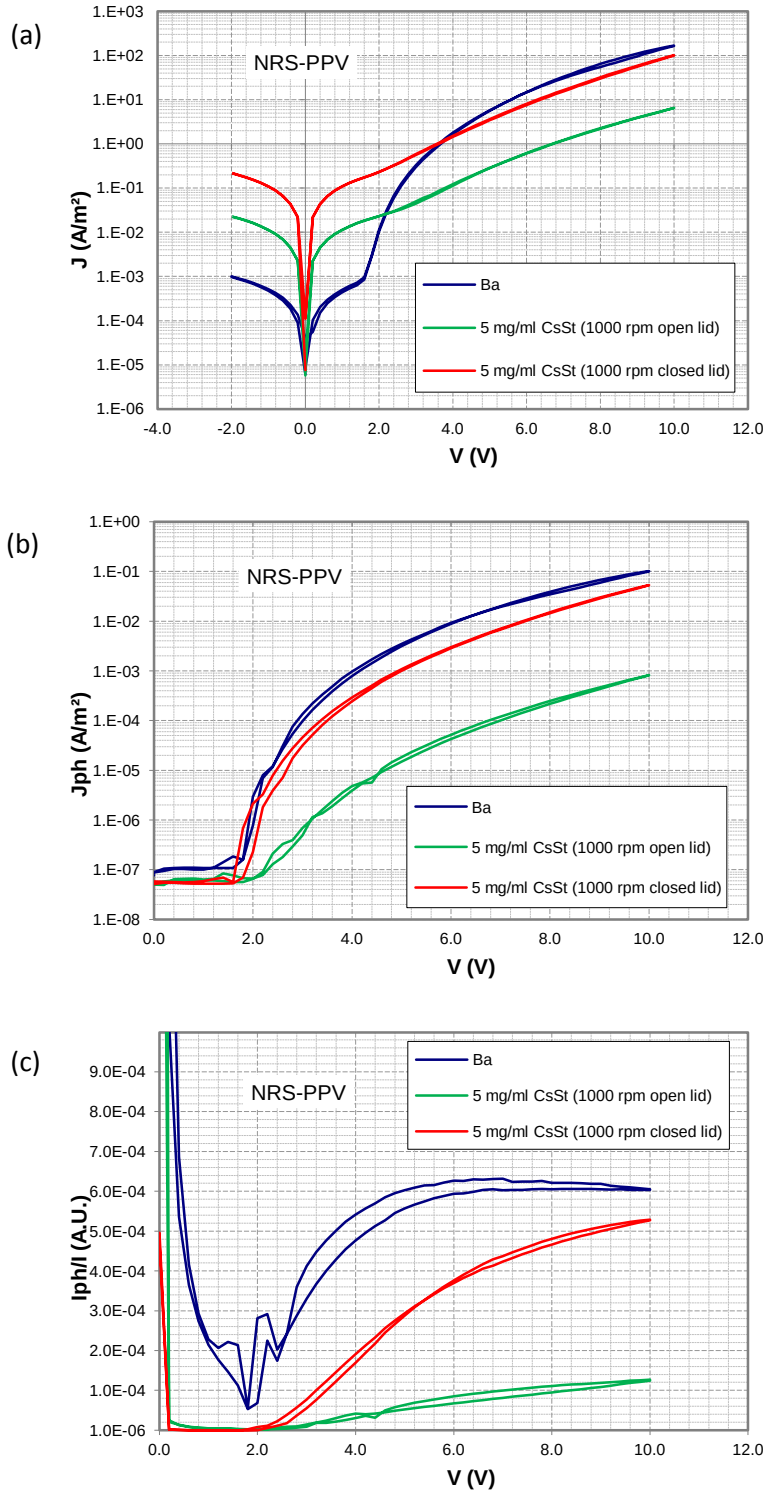

Figure 4.2. (a) J-V characteristics of OLEDs consisting 150 nm NRS-PPV (active layer) with different programs of spin coating 5 mg/ml CsSt as a cathode at room temperature compared to the device with Ba cathode (blue line). The corresponding (b) photocurrent density and (c) efficiency of devices.

In the next step, in order to have an idea how the electron injection functions we replace the top metal contact (Al) with Ag to investigate if the mechanism of injection is related to the top contact material. We have chosen Ag because it has a work-function close to that of Al but it is much less chemically reactive. Al and Ag have been thermally evaporated with the thickness of 100nm and 80nm, respectively. 2 mg/ml CsSt was spin coated by 1000 rpm with closed lid. From the figure 4.3(c), the maximum efficiency of the device including Ag contact is ~10^{-5} and the efficiency of the Al top contact device is ~7.4×10^{-4}. Therefore, as results show [figure 4.3], this replacement gives rise to a huge reduction in light output and consequently less efficiency. Although the mechanism is not understood, this seems that CsSt could not inject electrons from the Ag to the active layer, significantly. It may concern with the effect of slightly difference between the work-function of contacts, which is evaluated to be ~4.3 for Al and ~4.6 for Ag, or this result may imply that an interaction between CsSt and Al at the interface plays important role in injection of electrons from Al to the emissive layer. Analogous results have been achieved in studies of cesiumcarbonate (Cs_2Co_3) material as a cathode in PLEDs [1-2]. Huang and co-workers have reported that the solution-processed Cs_2Co_3 forms an Al-O-Cs structure at the interface of Al contact, and they concluded that the reaction of Al with spin-coated Cs_2Co_3 is the origin of formation a low work-function interfacial layer and hence much effective injection is resulted [1]. In addition, recently, Zhao et al. have detected the diffusion of Al into the Cs_2Co_3 in their experiments and from the spectra of the Al XPS they recognized an interaction between Al and Cs_2Co_3 [2]. Moreover, in the studies of thermally evaporated Cs_2Co_3, it has been demonstrated that however the main mechanism of injection is ascribed to the decomposition of Cs_2Co_3 during the vapor deposition, the reaction of thermally evaporated Cs_2Co_3 with Al can further reduce the work-function of the cathode and improve the injection process [1, 3 and 4].

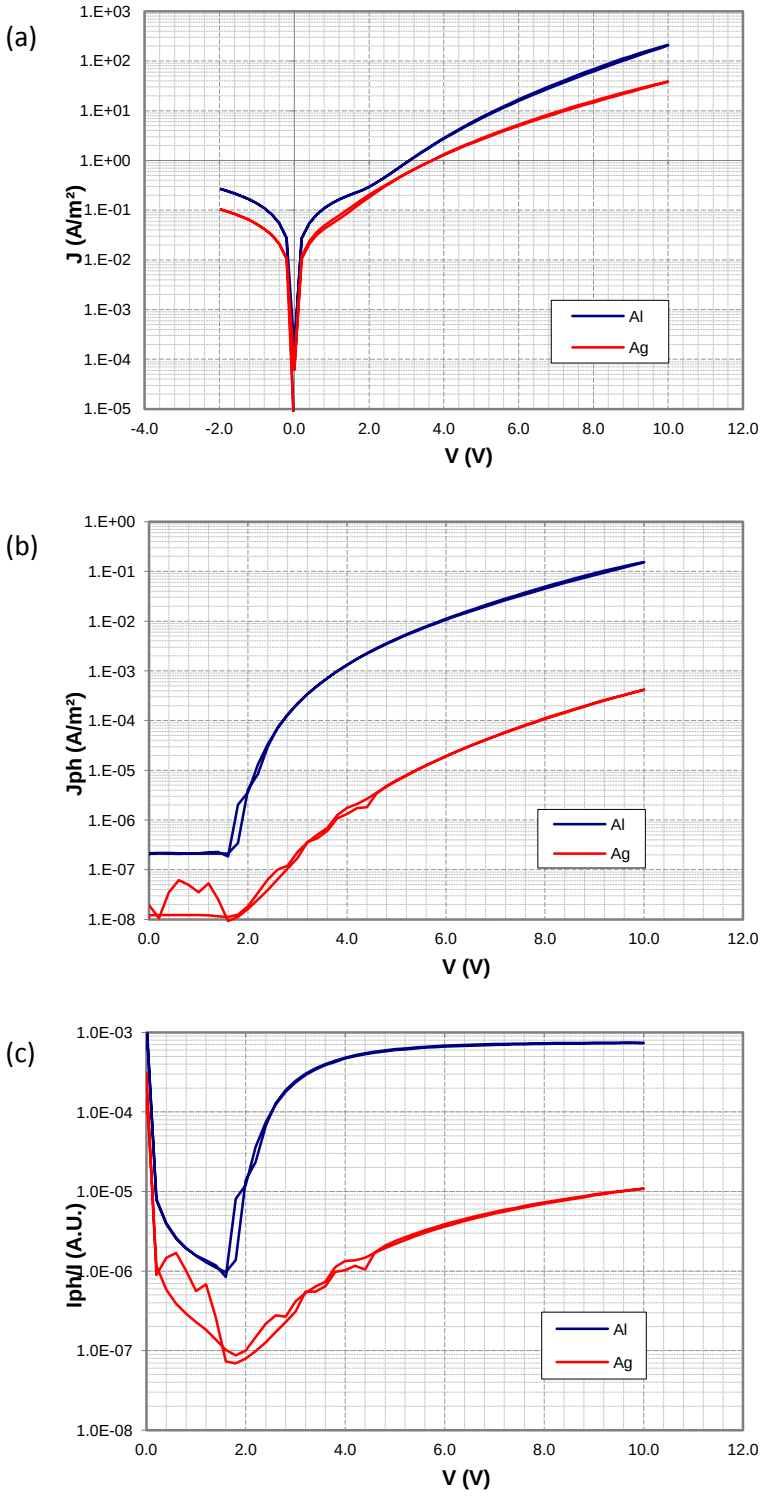

Figure 4.3. (a) The comparison of J-V characteristics of OLEDs consisting 150 nm NRS-PPV (active layer) with CsSt as a cathode and different top contacts; Al (blue line) and Ag (red line), at room temperature. The corresponding (b) photo current density and (c) efficiency of devices.

In the following an other derivative of PPV polymer called poly(2-methoxy-5-(2′-ethylhexoxy)-1,4-phenylenevinylene)(MEH-PPV) is investigated. MEH-PPV differ from NRS-PPV by it's side-chain and has almost the same band gap which results in red/orange emission. So, for this material spin coating of 2mg/ml CsSt with 1000 rpm revealed the best result as well. This result of MEH-PPV based device with the thickness of 145 nm is compared with that of reference device in figure 4.4. As can be seen from the figure 4.4(c) the efficiencies are in the same order of magnitude.

The emission spectrum of devices indicates no shifting, due to CsSt cathode, occurs in color emission [figure 4.5].

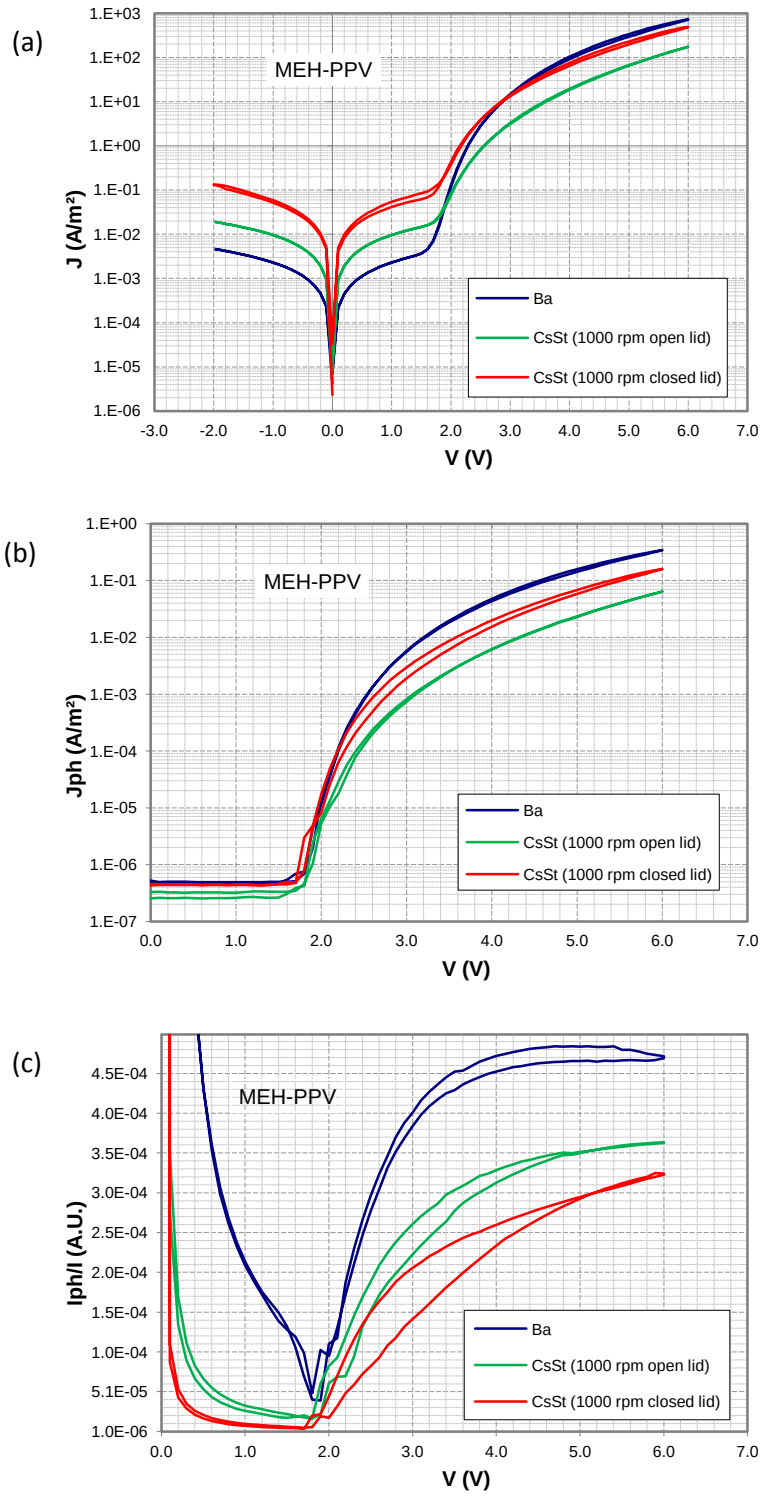

Figure 4.4. (a) J-V characteristics of OLEDs consisting 145 nm MEH-PPV (active layer) with different programs of spin coating 2 mg/ml CsSt as a cathode at room temperature compared to the device with Ba cathode (blue line). The corresponding (b) photocurrent density and (c) efficiency of devices.

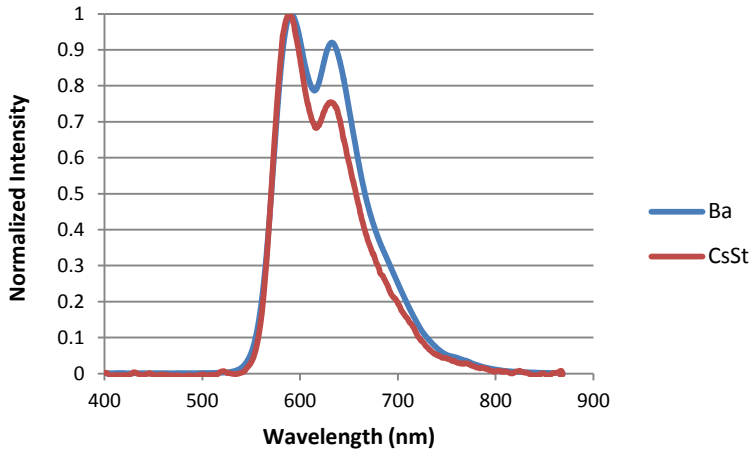

Figure 4.5. Emission spectra of 145 nm MEH-PPV based OLEDs with different cathode; Ba cathode (blue line) and CsSt cathode (red line), recorded at 5 V.

In order to compare the lifetime of devices with the Ba based device, the samples were kept inside the nitrogen-filled glovebox and after 4 days the current density was measured. The efficiencies were in the same magnitude as before but a lot of dark spots were created on the shining areas. Then the samples were taken out of nitrogen-filled glovebox, on day 6, and were characterized in the room atmosphere several times in a day with 2 hours duration in between. The efficiencies still were almost the same as before in magnitude but more dark spots were observed in the lighting areas. The measuring was continued and 2 days later, only some spots were lightening in the reference device (they may resemble the created short currents due to the numerous operation) and slightly larger parts were shining in the under study devices. These results are shown in figures 4.6, 4.7 and 4.8. From these observations, it seems that the degradation mechanism of samples is different, as the Ba based device degrades faster in terms of current and luminance while the CsSt based OLEDs degrade faster in terms of efficiency.

In this respect, the use of air-stable charge-injection interfaces is of particular importance. Recently, metal oxides have gained interest for this purpose. In fact, metal oxides are considered as a good candidate since they bring forward the combination of criteria such as good electrical conductivity, high transparency, ability of depositing on large areas as well as high air stability. The high performance devices reported with this point of view are those which consisting of both a metal oxide cathode and anode [5-10]. In these devices, actually, the organic emissive material is sandwiched between two metal oxide electrodes and the device is protected from the environment. Such a kind of

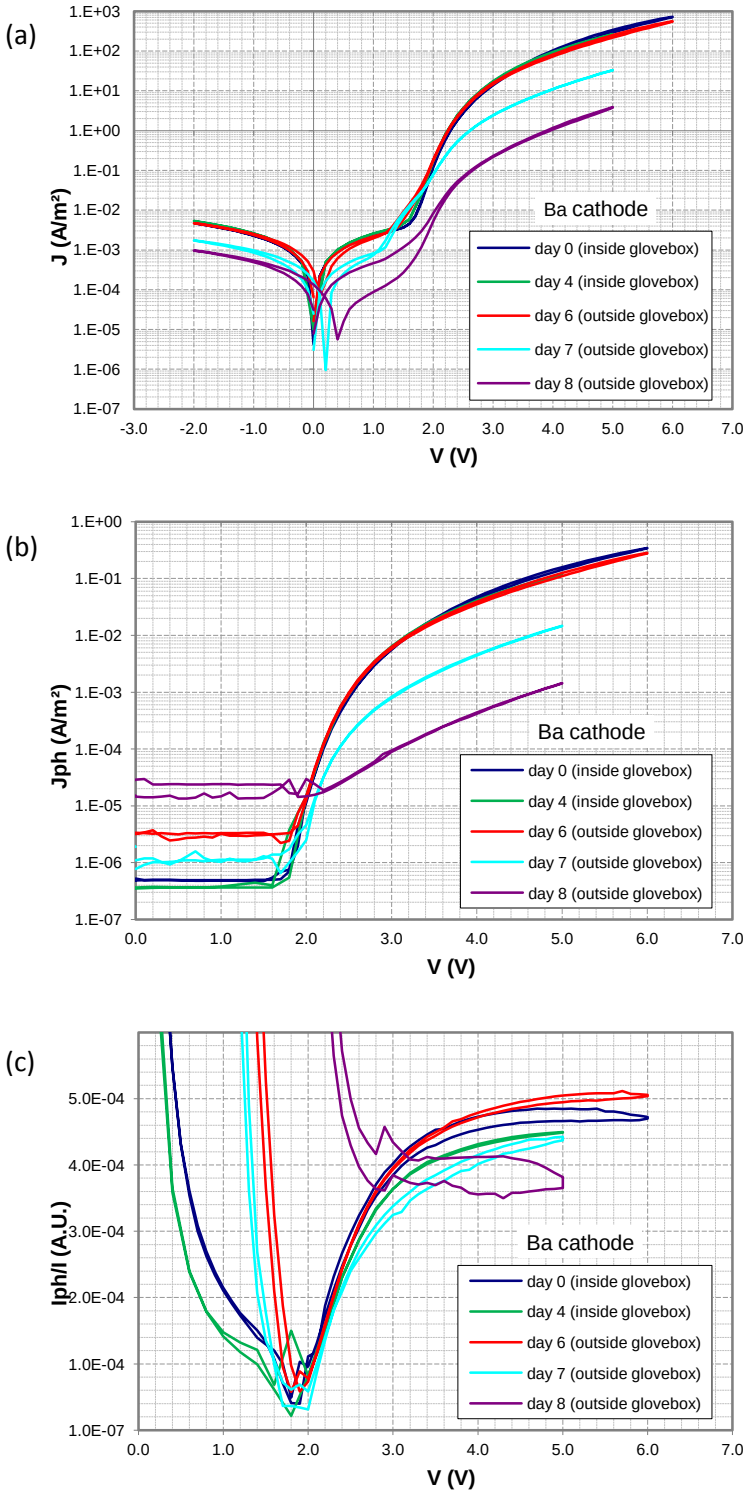

Figure 4.6. Stability of an OLED consisting 145 nm MEH-PPV (active layer) with Ba cathode. (a) J-V characteristics, and the corresponding (b) photocurrent density and (c) efficiency of device.

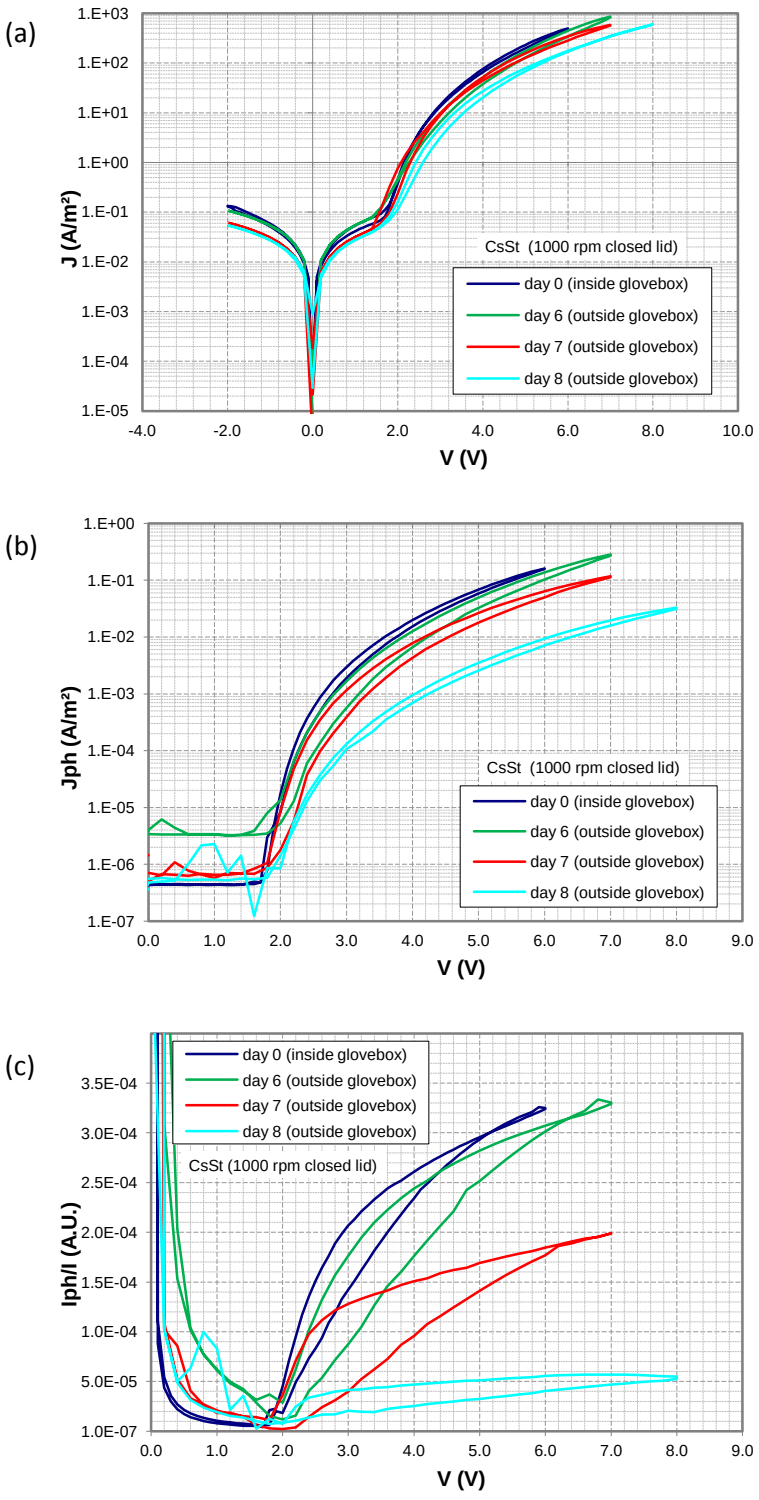

Figure 4.7. Stability of an OLED consisting 145 nm MEH-PPV (active layer) with CsSt as a cathode spin coated with closed lid. (a) J-V characteristics, and the corresponding (b) photocurrent density and (c) efficiency of device.

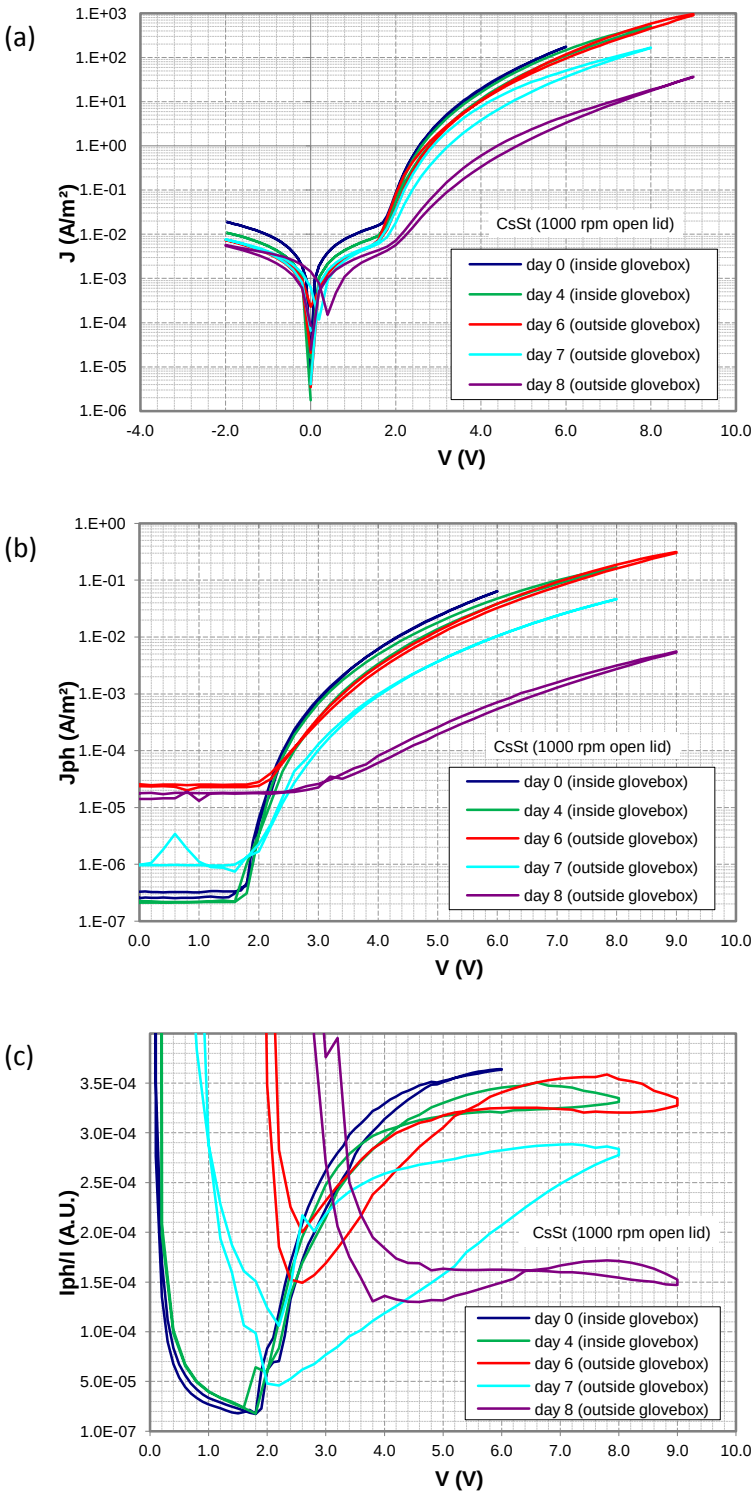

Figure 4.8. Stability of an OLED consisting 145 nm MEH-PPV (active layer) with CsSt as a cathode spin coated with open lid. (a) J-V characteristics, and the corresponding (b) photocurrent density and (c) efficiency of device.

OLEDs are known as hybrid organic-inorganic light-emitting diodes (HyLEDs) having the advantages of both organic and inorganic materials with inverted architecture compared to conventional ones. In an inverted structure, the cathode is deposited on top of bottom contact and anode is placed on top of active layer. Examples of metal oxides used in this field are molybdenum trioxide (MoO_3) and vanadium pentoxide (V_2O_5) as hole injectors, zinc oxide (ZnO) and titanium oxide (TiO_2) as electron injectors. As a cathode, ZnO exhibits a low work-function and, more recently, Bruyn et al. have demonstrated that ZnO is as efficient as Ba in conventional OLEDs and provides exceptional stability [5]. Furthermore, in Ref [6] Lu and coworkers have provided better alignments between work-function of ZnO and the LUMO level of several polymers including MEH-PPV, Poly[9,9-didecanefluorene-alt-(bis-thienylene)benzothiadiazole] (PF10TBT) and an indacenodithiophene copolymer with a benzothiadiazole acceptor unit (IDTBT) by electrical conditioning which resulted in a comparable efficiency of the inverted OLED with the normal geometry OLED. They have attributed this observation to the processing conditions of ZnO that they used in their experiments which leads to accumulation of hole carriers at the interface of ZnO/polymer. Other report shows efficient electron injection can be achieved by ZnO in a F8BT based HyLED [7]. Afterwards, it was shown that electron injection into the F8BT was improved by modifying the ZnO surface using Cs_2Co_3 [8]. A thin layer of solution-processed Cs_2Co_3 in contact with ZnO leads to not only a decrease in substrate work-function, but also an interfacial n-doping of the polymer by the Cs_2Co_3 [8-9]. Later on, further improvement was revealed in the report of Vaynzof et al. via coannealing of the Cs_2Co_3 and the F8BT films [10].

In this work, with the same purpose, we employed CsSt material to enhance the electron injection from ZnO into the MEH-PPV, although, unfavorable result is obtained [Figure 4.9].

ZnO was dissolved in ethanol from a precursor solution of Zinc acetyl acetonate hydrate ($Zn(acac)_2$) with the concentration of 20 mg/ml followed by conversion to ZnO at 55℃. To fabricate inverted OLEDs, ITO patterned substrates were heated at 55℃ for few minutes and a layer of ZnO was spin coated in ambient condition yielding layer thickness of 20 nm. After annealing the samples at 120℃ for 1 minute, they were transferred into the nitrogen-filled glovebox and 2 mg/ml CsSt was spin coated at 1000 rpm rate in the case of under investigation device. Active layer (MEH-PPV) was deposited and fabrication procedure was followed by evaporating a 10 nm MoO_3 layer encapsulated by 100 nm Al layer under pressure of 10^{-6} mbar. Our result which belongs to ordinary inverted device (without CsSt layer) is in consistent with the result of Ref [6].

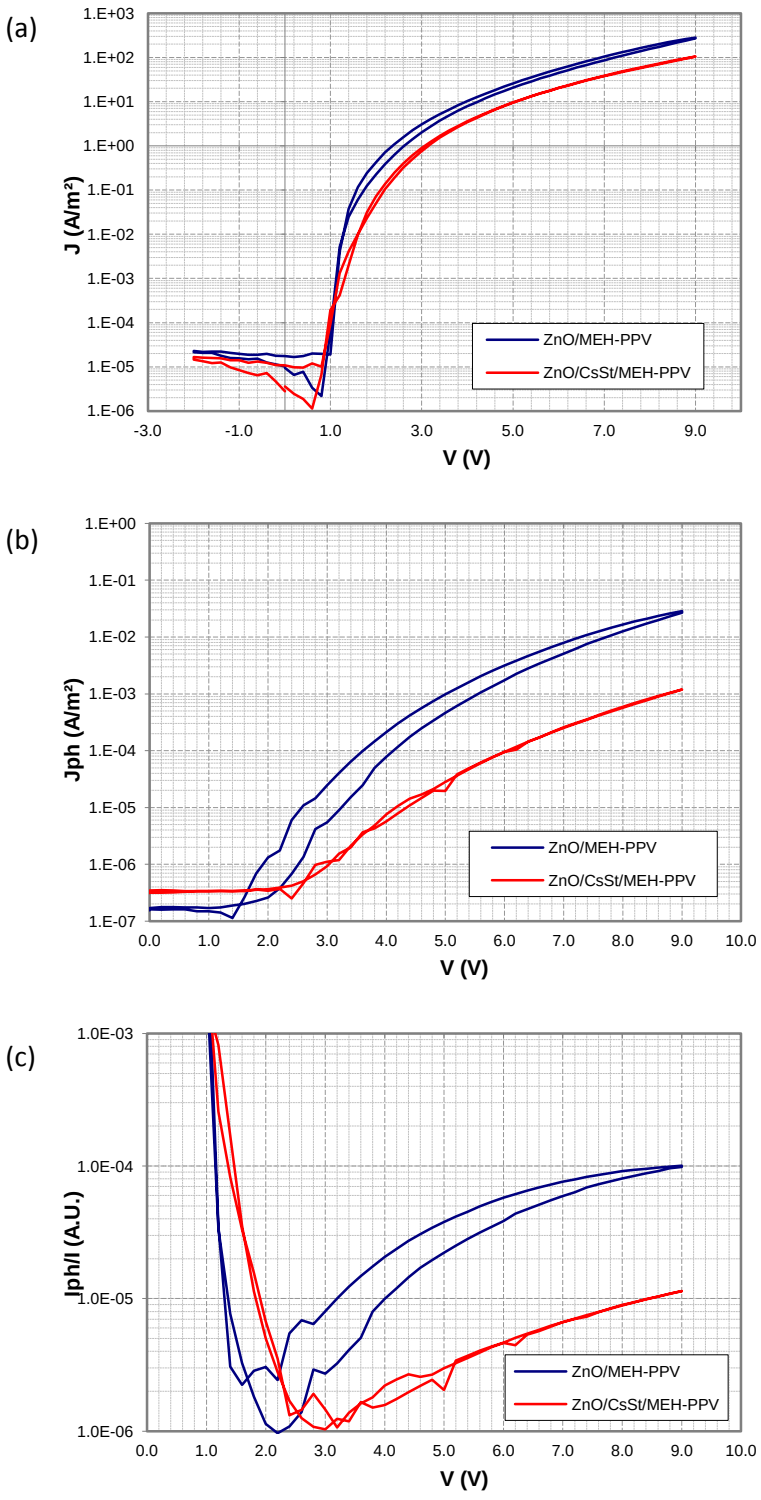

Figure 4.9. Comparison of (a) current density, (b) photocurrent density and (a) efficiency of an ITO/ZnO/CsSt/MEH-PPV/MoO_3/Al inverted structure device with ordinary inverted OLED (ITO/ZnO/MEH-PPV/MoO_3/Al). Thickness of active layer is 170 nm.

In order to investigate the electron injection property of CsSt more precisely, electron only (EO) devices were prepared. All devices were constructed on glass substrates on which a layer of Al with the thickness of 30 nm was evaporated. Depending on the cathode material which would be investigated as either a bottom or top contact, different layers were deposited subsequently, finally, all the devices were encapsulated by 100 nm Al. The active material was 140 nm MEH-PPV.

The electron injection characteristic of CsSt was investigated by the structures of Al/CsSt/MEH-PPV/Al and Al/MEH-PPV/CsSt/Al as a bottom design cathode and top configuration cathode, respectively. As figure 4.10 shows, CsSt acts as a somewhat more efficient cathode when it is deposited on the bottom contact. Hysteresis curves in the plots are the feature of EO devices; that is probably due to permanent trapping of electrons.

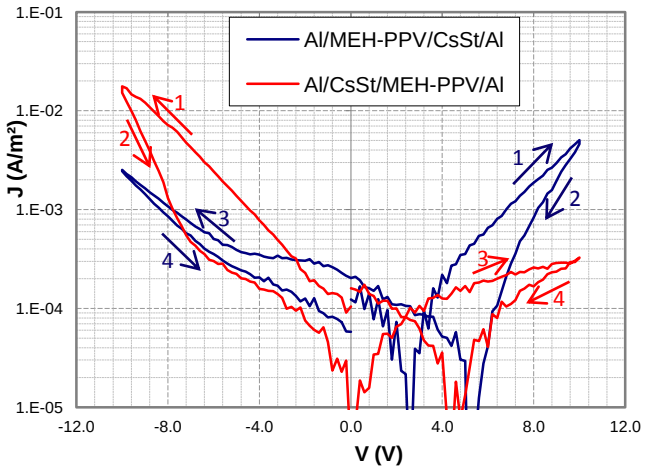

Figure 4.10. J-V characteristics of EO diodes with different structures. The Blue plot corresponds to the structure where CsSt is used on top of active layer and the red plot is for the device in which CsSt is used as a bottom electrode.

The electron injection ability of bottom design CsSt cathode is compared with that of Ba in figure 4.11. The curves show electron injection of CsSt is comparable to that of Ba (the difference is by a factor of 7) when the backward bias is applied. Dealing with EO diodes, it is necessary that the fresh samples to be tested, so slightly difference can be seen in the currents when switching inversely.

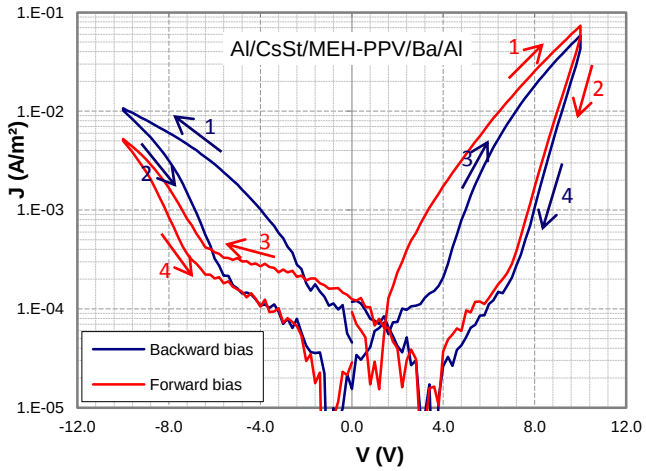

Figure 4.11. J-V characteristics of EO diodes with structure of Al/CsSt/MEH-PPV/Ba/Al under applying forward and backward biases.

By considering the hypothesis that the bottom design CsSt acts as a better injector together with the fact that the electron barrier is smaller where the Al is used as a bottom contact [11], we aimed to study an inverted OLED in which the ZnO is replaced by a thin layer of Al. The thickness of Al was chosen to be 5 nm. For comparison, the result of ordinary inverted OLED (ZnO/MEH-PPV) is also presented. Consider the blue and red curves in figure 4.12, although it is not completely clear if the injection would not be problematic, we believe that the lower photocurrent may stems from the fact that 5 nm Al was not transparent enough to allow the light to escape from the device. Hence, a device with 2 nm Al was considered. In this case for sure there is not sufficient electron to recombine with holes, since the measurements reveal lower photocurrent with respect to the device with 5 nm Al despite of the fact that 2 nm Al is more transparent. In conclude no reasonable results were achieved by this new suggestion of inverted OLED configuration, because having effective electron injector and transparent electrode simultaneously cannot be provided by Al.

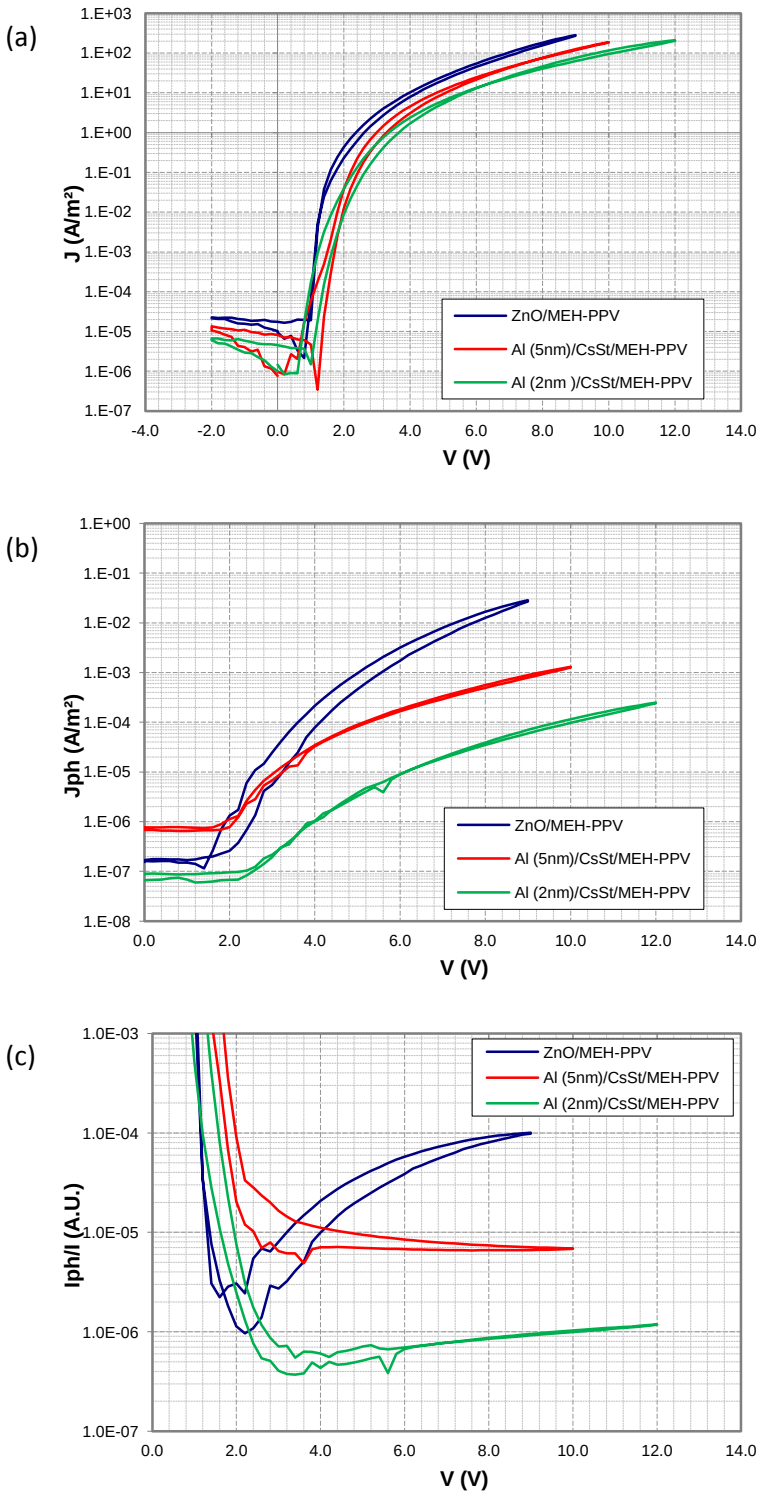

Figure 4.12. Comparison of (a) current density, (b) photocurrent density and (c) efficiency of ITO/Al/CsSt/MEH-PPV/MoO_3/Al inverted structure devices with ordinary inverted OLED (ITO/ZnO/MEH-PPV/MoO_3/Al).

4.2.2 Charge injection and recombination in blue polymers: SPB001-002 and SPB103-001

Blue emitting polymers have wide band gap which makes the injection to be complicated for both electrons and holes. In order to overcome this problematic issue, different approaches have been investigated in Ref [12] by Nicolai. One rout is the incorporation of arylamine units to improve the injection and transport of holes, as hole injection is understood to be more challenging due to the deep HOMO level of these polymers. SPB001-002 and SPB103-001, investigated blue emitting materials in this thesis, are two examples of such polymers with different amounts of hole transporting unit. Fist the results of SPB001-002 with 190 nm thickness are presented in figure 4.13. Here, the only reasonable result is given by spin coating of 1.5 mg/ml CsSt with 1000 rpm when the lid is open. However, interestingly enough, the efficiency of the case study device is slightly higher than that of reference, the lighting area was not uniform and random parts were shine which indicates that the CsSt cannot be coated smoothly on top of this polymer.

The other blue polymer, SPB103-001, is studied under different conditions of spin coating 2 mg/ml cathode material as well, and compared with reference device in figure 4.14. This polymer has a lower LUMO level with respect to the previous one leading to lower potential barrier for electrons and hence more efficient electron injection. This feature can also be observed by comparing the J-V and $J_{ph} - V$ plots of the two reference devices, where in the case of SPB103-001 based device the higher current acquired in lower voltages on one hand and the turn on voltage is lower on the other hand which demonstrates lower band gap.

Although, the two under investigation SPB103-001 based samples show lower currents in compared to the Ba based device, they exhibit comparable efficiencies in high biases. We ascribe the lower efficiency in low voltages to the higher leakage current of them. We would like to mention that the lighting areas were uniform and only very tiny dark spots were observed. The active layer thickness was 90 nm.

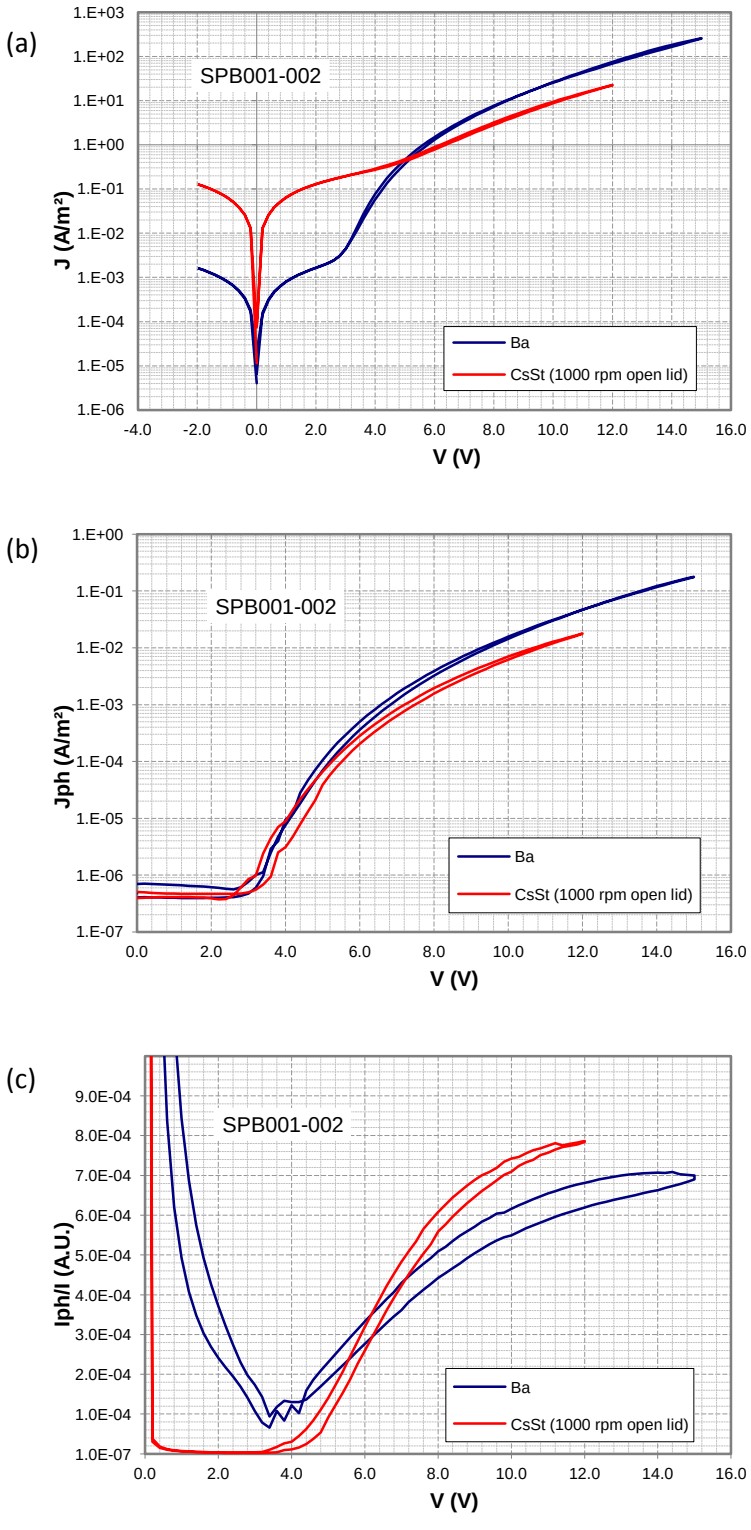

Figure. 4.13. (a) J-V characteristics of OLEDs consisting 190 nm SPB001-002 (active layer) with 1.5 mg/ml CsSt as a cathode, compared to the device with Ba cathode (blue line). The corresponding (b) photocurrent density and (c) efficiency of devices.

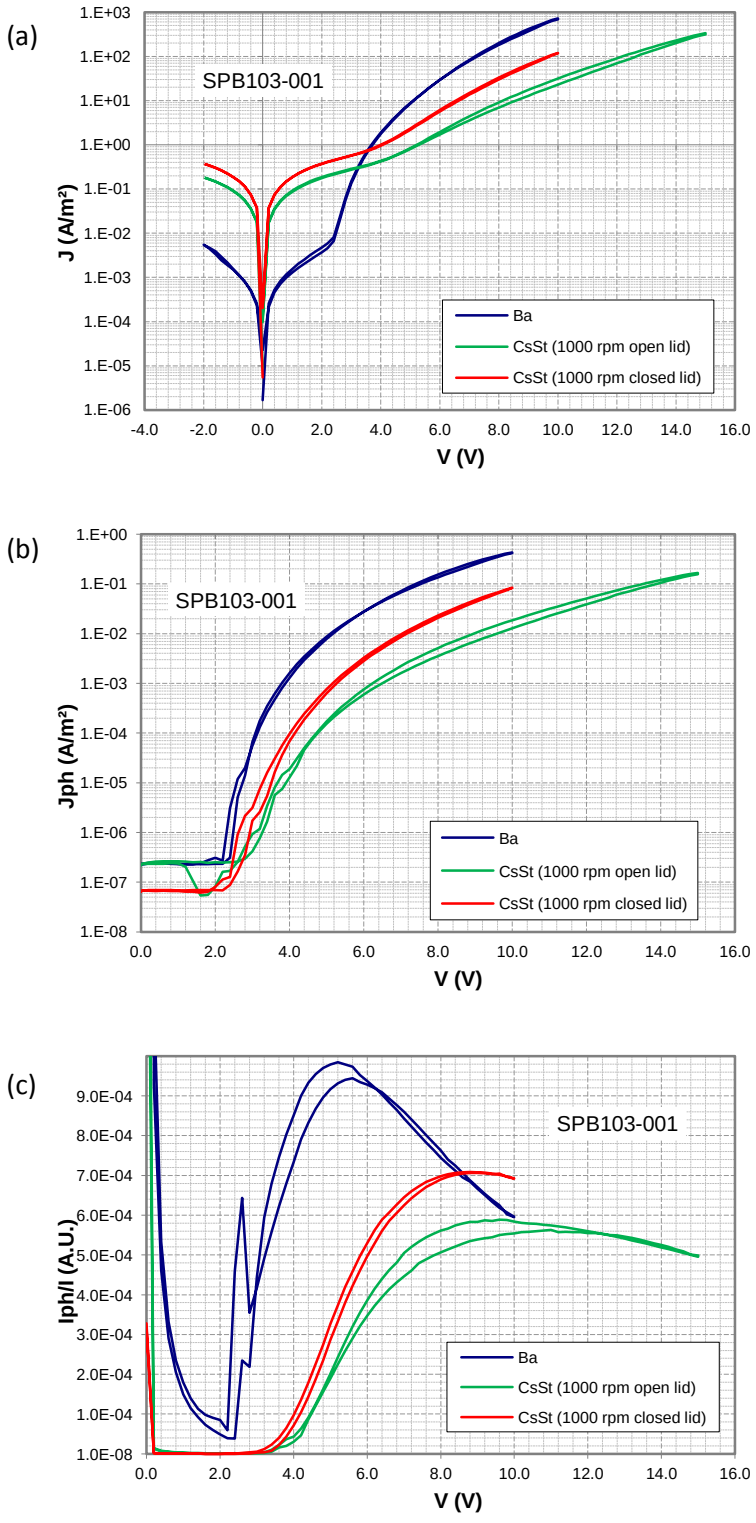

Figure. 4.14. (a) J-V characteristics of OLEDs consisting 90 nm SPB103-001 (active layer) with different programs of spin coating 2 mg/ml CsSt as a cathode, compared to the device with Ba cathode (blue line). The corresponding (b) photocurrent density and (c) efficiency of devices.

4.2.3 Charge injection and recombination in white copolymer: SPW106

The devices in this section are based on a 90 nm active layer of white emitting copolymer in which green and red dyes are incorporated in a blue backbone. Therefore, due to the wide band gap associated with blue backbone polymer, finding suitable injection materials is challenging. From the figure 4.15, it is clear that the current densities are quite low but the efficiencies are good enough and comparable to each other in high operation voltages. As mentioned before, the lower efficiencies of devices based on 2 mg/ml CsSt cathode (coated by 1000 rpm either with open or close lid) in low voltages attributed to the higher leakage current in comparison to reference device. It is worth to point that the active areas were uniform with very tiny dark spots in all devices.

Seeking to know the reason of low current feature of the devices, we investigated hole only (HO) devices with the structure of ITO/PEDOT-PSS/SPW106/MoO_3/Al, because, deep HOMO level is known as the characteristic of this copolymer and it has been proved that MoO_3 acts as a more efficient hole injector in polyfluorene derivatives, the class of materials which used as a backbone here [12]. In conclusion, figure 4.16 temperature scan of J-V measurements demonstrates no crucial difference between injections in terms of PEDOT-PSS and MoO_3. The scans are performed in forward bias. The hole mobility, $\mu_0 \sim 10^{-15}$ m^2/Vs, is determined few order of magnitudes lower than common luminescent polymers in this class of polymers. So, it may conclude that this copolymer is not a good conductor intrinsically.

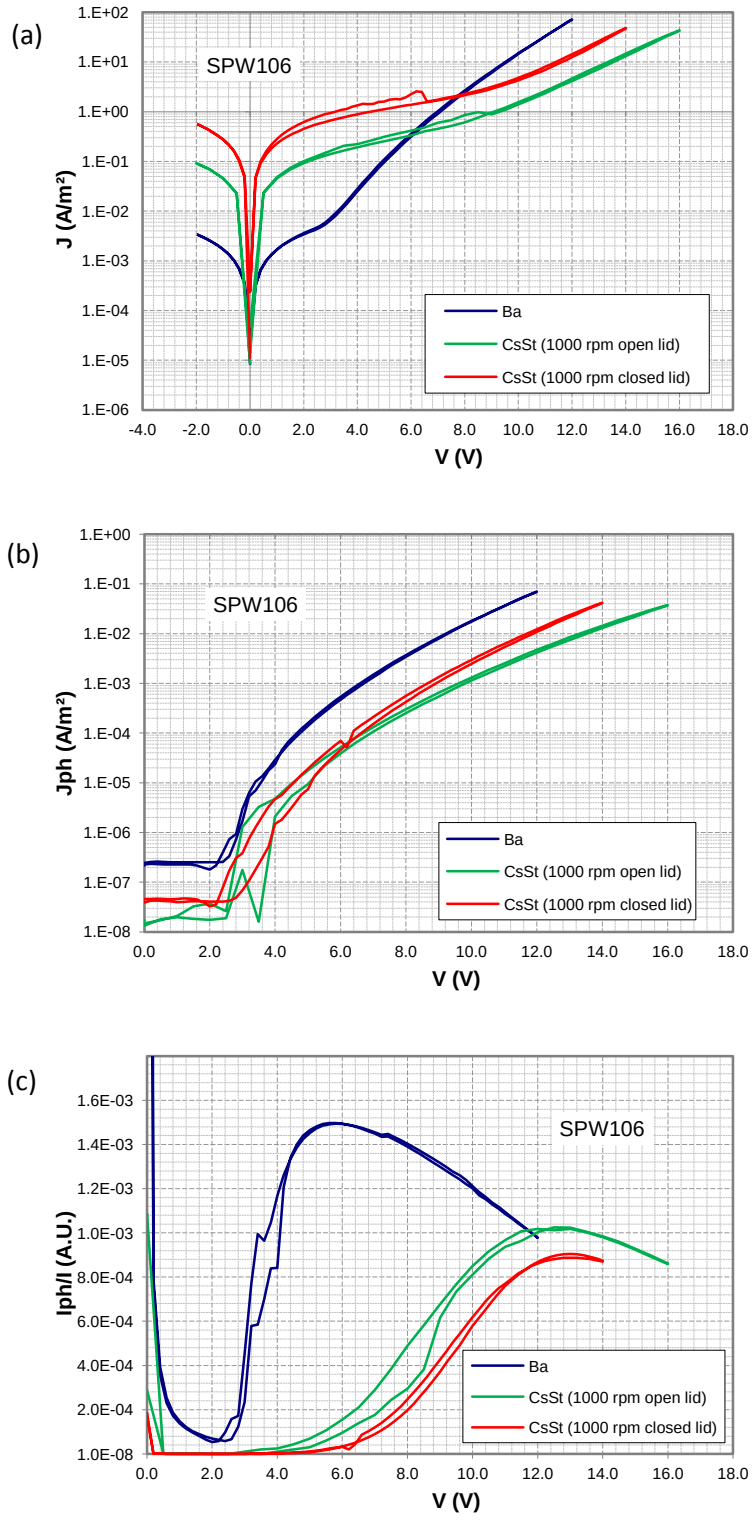

Figure. 4.15. (a) J-V characteristics of OLEDs consisting 90 nm SPW106 (active layer) with different programs of spin coating 2 mg/ml CsSt as a cathode, compared to the device with Ba cathode (blue line). The corresponding (b) photocurrent density and (c) efficiency of devices

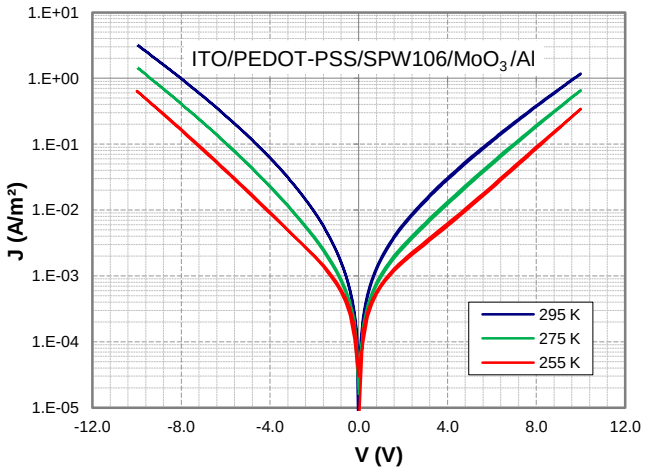

Figure 4.16. Temperature dependent J-V measurements of HO device with the structure of ITO/PEDOT-PSS/SPW106/MoO_3/Al.

4.3 Electron transport in polyfluorene derivative: LP121 F4

One of the loss mechanisms that suppress the luminescence in the OLEDs is exciton quenching at the cathode. In this line, multilayer OLEDs are interesting; however solution-processed multilayer devices remain problematic. In this work, a double layer solution-processed OLED is shown using an electron transporting polymer known LP121 F4. The LP121 F4 polymer supplied by MAX-PLANCK institute is a polyfluorene (PF) derivative with the chemical structure of figure 4.17 which is soluble in polar solutions. The polymer was spin coated from ethanol with the concentration of 9 mg/ml. The program used for coating is 1000 rpm with closed lid, yielding ~20 nm thickness of layer measured by AFM. This polymer is used as an electron transporting material between Ba and the active material which is 185 nm MEH-PPV. As depicted in figure 4.18 the results of the device are the same as what we get from the reference device. The extra electron transporting layer did not increase the efficiency. This unexpected result may be justified with the discussion of Ref [13] where the authors have investigated two different thicknesses of MEH-PPV OLEDs and quantitatively studied the effect of two different loss mechanisms; non-radiative trap-assisted recombination and exciton quenching at the cathode. They realized that for devices thicker than 100 nm, non-radiative trap-assisted recombination is the dominant current efficiency loss mechanism rather than quenching effects.

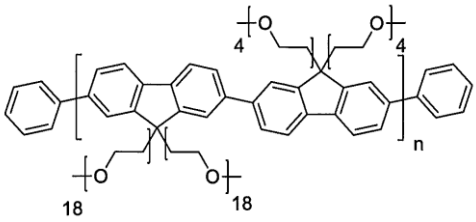

Figure 4.17. Chemical structure of LP121 F4 polymer**.**

We were interesting to know how the electron transporting layer would affect the results when it is used in the device without Ba cathode. Interestingly enough, the results were considerably comparable with that of reference device, indicating that electron injection into the polyfluorene electron-transporting layer is efficient even from an aluminum cathode. All the devices were different from each other slightly only at high voltages; however the lighting areas of devices including electron transporting layer exhibited some dark spots which were even larger dark parts in the case of single layer device with PF derivative layer.

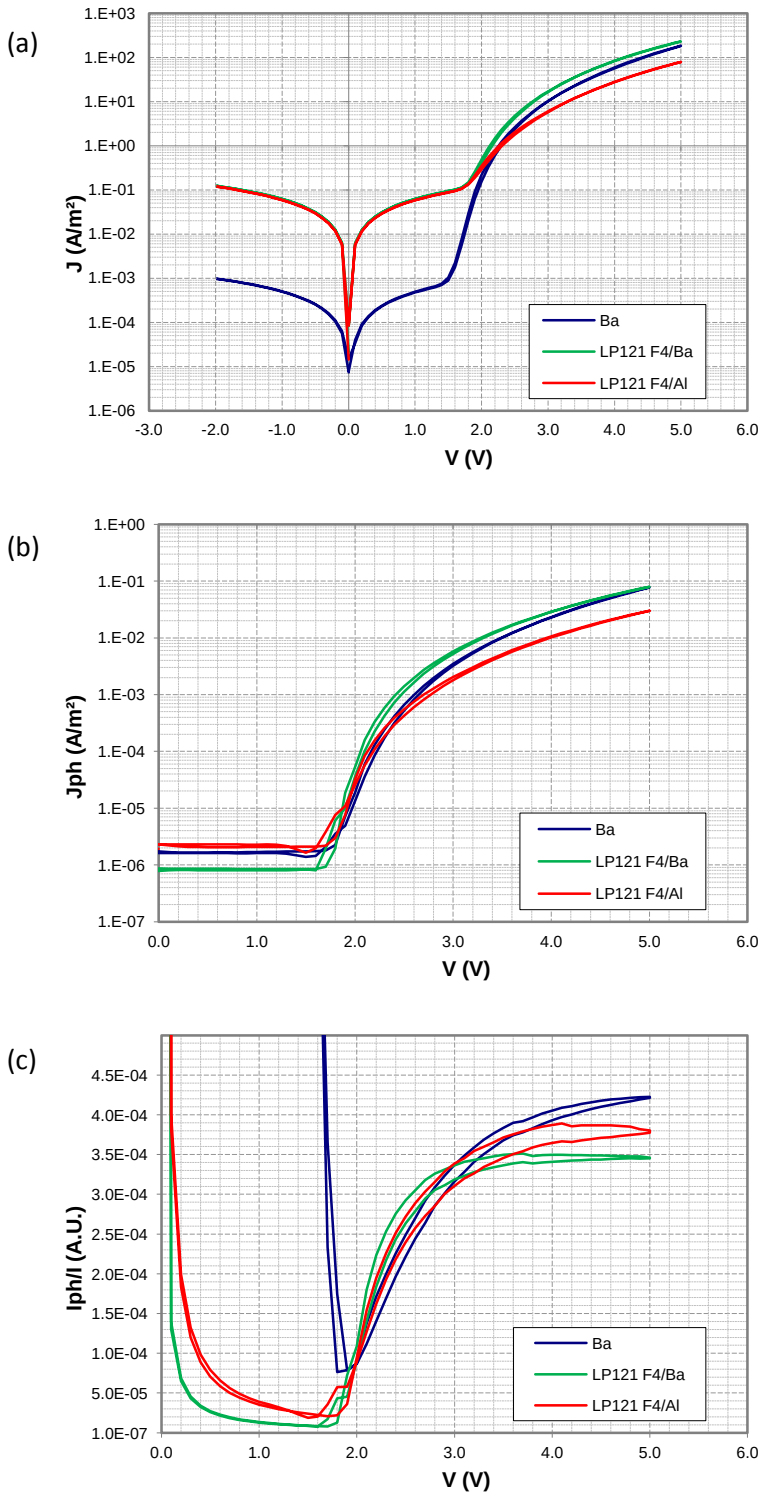

Figure. 4.18. (a) J-V characteristics of OLEDs consisting 20 nm electron transporting layer with the structure of ITO/PEDOT-PSS/MEH-PPV/LP121-F4/Ba/Al (green line) and ITO/PEDOT-PSS/MEH-PPV/LP121-F4/Al (red line). compared to the device with Ba cathode (blue line). The corresponding (b) photocurrent density and (c) efficiency of devices.

4.4 Conclusions

In conclusion, solution processable OLEDs were investigated in this work. An electron injector material called caesium stearate (CsSt) was introduced as a cathode which can be deposited through spin coating method and can replace conventional cathode layers deposited by thermal evaporation under high vacuum. The electron injection property of CsSt layer was investigated precisely using electron only diodes and it is shown that CsSt can be as efficient as Ba cathode. This result is also evident from the observations of a broad series of electrical measurements in different regions of spectrum (red/ blue/ white emitting active layers) presenting comparable device performances with that of evaporated Ba cathode based OLEDs. These results enable us to render fully solution processed OLEDs.

Study of devices fabricated with different encapsulating contact layer showed that electron injection from CsSt layer is relatively sensitive to the choice of capping metal. Moreover, comparison of lifetime of devices with reference one, which is a Ba based device, implies different degradation mechanism of samples.

In addition, a brief study was done on a solution processed double layer OLED together with a single layer one consisting an electron transporting layer. Although the results of single layer device had good agreements with the results of reference device, we believe that CsSt is better option for solution-processable cathode purposes, since it can be reproduced much easier than polyfluorene derivative polymer that used here as electron transporting layer.

References

[1] J. Huang, Zh. Xu, and Y. Yang, Adv. Funct. Mater., 17, 1966, (2007).

[2] Y. Zhao, L. Duan, D. Zhang, L. Hou, J. Qiao, L. Wang, and Y. Qiu, Appl. Phys. Lett., 100, 083304 (2012).

[3] Ch-I Wu, Ch-T Lin, Y-H Chen, and M-H Chen, Y-J. Lu, and Ch-Ch. Wu, Appl. Phys. Lett. 88, 152104, (2006).

[4] Y. Li, D-Q. Zhang, L. Duan, R. Zhang, L-D. Wang, and Y. Qiu, Appl. Phys. Lett. 90, 012119, (2007).

[5] P. de Bruyn, D.J.D. Moet, and P.W.M. Blom, Organic Electronics, 13, 1023, (2012).

[6] M. Lu, P. de Bruyn, H. T. Nicolai, G-J. A.H. Wetzelaer, and P. W.M. Blom, Organic Electronics, 13, 1693, (2012).

[7] H. J. Bolink, E. Coronado, D. Repetto, and M. Sessolo, Appl. Phys. Lett. 91, 223501, (2007).

[8] D. Kabra, L. P. Lu, M. H. Song, H. J. Snaith, and R. H. Friend, Adv. Mater., 22, 3194, (2010).

[9] H. J. Bolink, E. Coronado, J. Orozco, and M. Sessolo, Adv. Mater., 21, 79, (2009).

[10] Y. Vaynzof, D. Kabra, L. L. Chua, and R. H. Friend, Appl. Phys. Lett., 98, 113306, (2011).

[11] M. M. Mandoc, B. de Boer, and P. W. M. Blom, Phys. Rev. B, 73, 155205, (2006).

[12] H. T. Nicolai, Zernike Institute PhD thesis, ISBN: 978-90-367-5398-2 (Electronic version), (2012).

[13] M. Kuik, L.J.A. Koster, A.G. Dijkstra, G.A.H. Wetzelaer, and P.W.M. Blom, Organic Electronics 13, 969, (2012).

Acknowledgements

I would like to appreciate all the people whose support was invaluable during my master project. I gratefully acknowledge Prof. Blom who kindly let me to have the opportunity of working in his group. Special thanks go to Gert-Jan, my daily supervisor, who I learned a lot from him and he was patient enough to answer my naive questions. I would like to thank Jan Harkema for his invaluable technical help and assistance. Also I would like to say thanks to whole ME-POS group members who I learned many new things from them during our discussions in group meetings, people who made such a great friendly atmosphere and I enjoyed a lot with them. I acknowledge financial support from the Zernike Institute for Advanced Materials which making my master studies possible at the University of Groningen.